Journal of the Mechanics and Physics of Solids 134 (2020) 103752

Contents lists available at ScienceDirect

Journal of the Mechanics and Physics of Solids

journal homepage: www.elsevier.com/locate/jmps

An analysis driven construction of distortional-mode-dependent and Hill-Stable elastic potential with application to human brain tissue

Durga Prasad, K. Kannan[1,*]

Department of Mechanical Engineering, Indian Institute of Technology Madras, Chennai 600036, India

ARTICLE INFO

Article history:
Received 1 July 2019
Revised 26 August 2019
Accepted 7 October 2019
Available online 7 October 2019

Keywords:
Human brain tissue
Lode invariants
Shear superposed on uniaxial deformation
Hyperelasticity
Construction of potential
Baker-Ericksen inequality
A priori analysis
Hill inequality
True-stress-True-Strain monotonicity
Strong ellipticity
Mihai-Ogden model
Empirical inequality

ABSTRACT

We propose an innovative procedure by exploiting the physical meaning of natural strain or Lode invariants with the following salient contributions: 1) Uniaxial data for human brain tissue is used to stipulate the mathematical structure of the potential in terms of the Lode invariant that quantifies the magnitude of distortion along with the modulus term being an unknown function of the Lode angle that quantifies the mode or type of distortion. 2) By *a priori* analysis using the Baker-Ericksen inequalities, the mathematical form of the modulus function is determined in a novel manner. 3) The derived modulus function is corrected by adding a constant, which in turn is determined using analysis involving sufficient conditions of the stronger Hill inequality. 4) In addition, we also prove that any potential that satisfies Hill inequality also satisfies true-stress-true-strain monotonicity condition in plane stress. Compared to Mihai-Ogden model, besides excellent quantitative agreement with data for human brain tissue (see Mihai et al., 2017), the constructed model also emulates the observed non-linear behavior of shear stress with respect to the amount of shear as opposed to the nearly linear response predicted by the antecedent model. Additionally, when only tension-compression data is available for determining material parameters, the predicted combined tension and shear response associated with the proposed constitutive relation shows monotone decreasing Poynting stress (compressive), while the former predicts an unexpected non-monotone response for certain levels of tension.

1. Introduction

Many constitutive inequalities have been proposed for hyperelastic materials in the past, and not all of them enjoy the same status. We begin with a short analysis of various constitutive inequalities and their interrelation before describing the construction of an elastic potential because appropriate inequalities are required for scrutiny of contending mathematical forms that are suitable for constitutive relations.

The inequalities proposed by Baker and Ericksen (1954) state that the principal values of Cauchy stress and its corresponding stretches are ordered in the same manner. This physically reasonable inequality (B-E inequalities) is conceived by considering a homogeneous triaxial deformation of an isotropic elastic block. Rivlin (2004) superimposed an infinitesimal

* Corresponding author.
E-mail addresses: me14d059@smail.iitm.ac.in (D. Prasad), krishnakannan@iitm.ac.in (K. Kannan).
[1] Dedicated to my late father S.V. Kannan.

https://doi.org/10.1016/j.jmps.2019.103752
0022-5096/

simple-shear on the triaxial deformation considered by Baker and Ericksen (1954) and showed that the inequalities are both necessary and sufficient for the shear stress and the shear strain to be in the same direction or the incremental shear modulus to be positive. In related work, Mihai and Goriely (2011) showed that the deformation of any hyperelastic isotopic material subjected to pure shear can be decomposed into a triaxial state and simple shear in the direction of shear stress if and only if the B-E inequalities hold. By augmenting the connection of B-E inequalities with that of realistic physical behavior, Marzano (1983) showed that these inequalities are also necessary and sufficient for the simple tension to correspond to a simple extension. It appears that the mounting circumstantial evidence in favor of B-E inequalities led Neff et al. (2015) to comment that, and we quote, *the Baker-Ericksen inequalities are arguably an absolutely necessary requirement for reasonable material behaviour*.

Now we turn our attention to stronger constitutive inequalities which imply B-E inequalities. Accordingly, the constitutive inequalities such as E-inequalities, strong ellipticity and Hill inequality are scrutinized. For an incompressible, isotropic and hyperelastic material undergoing uniform shear, Mihai and Goriely (2011) have shown that imposition of E-inequalities (refer to Truesdell and Noll, 2004) leads to positive Poynting effect. Measurements made by Balbi et al. (2019) also showed that brain tissue exhibits positive Poynting effect. However, Truesdell's empirical or E-inequalities also imply ordered forces (O-F) inequality, which may be violated for nearly incompressible and incompressible isotropic elastic materials, as demonstrated by Sidoroff (1974) and Rivlin (2004). Therefore, E-inequalities are not appropriate for the human brain tissue which is nearly incompressible.

Strong ellipticity is connected with the existence of real wave speeds in the linearized theory of elasticity, in that, real wave speeds imply strong ellipticity (see Marsden and Hughes, 1994). That strong ellipticity may be desirable, but the loss of the same is **not a mathematical pathology** was expounded by Silhavy (2013): *They are related to the qualitative features of the equilibrium states, like their existence/nonexistence, stability/instability, uniqueness/nonuniqueness, the occurrence/nonoccurrence of phase boundaries, etc. Moreover, the violation of these and other 'mathematically desirable' features is now understood not as a mathematical pathology, but as a sign indicating (the possibility of) an interesting physical phenomenon, phase transition, observable large- or fine-scale instability of another 'catastrophic' feature.* In order to substantiate the assessment made by Silhavy, we draw the readers attention to the work of Knowles and Sternberg (1976) and Abeyaratne (1980). They show that the loss of ellipticity of equilibrium equations is necessary for the existence of elastostatic shocks, i.e., fields with continuous displacement and discontinuous displacement gradients for compressible, isotropic and hyperelastic materials under plane strain and its corresponding counterpart belonging to the incompressible class, respectively. In a connected effort, Zee and Sternberg (1983) obtained necessary and sufficient conditions for strong ellipticity explicitly in terms of the stored energy function in a three dimensional setting for the incompressible class. They also demonstrate for special stored energy functions that the loss of monotonicity of shear stress in simple shear coincides exactly with the loss of ellipticity mirroring the findings of Abeyaratne (1980). Recently (Zubov and Rudev, 2011) obtained necessary and sufficient conditions for strong ellipticity on the stored energy function in an easily tractable and verifiable form. However, there are difficulties in constructing an elastic potential using Hencky strain, which satisfies strong ellipticity conditions in the entire range of deformations. Martin et al. (2018) have shown that it is impossible to construct a potential that is both a monotone increasing function of $||\mathrm{dev}_n(\mathrm{Log}(\mathbf{V}))||$ for $n \geq 3$, where $\mathbf{V}$ is the square root of left Cauchy-Green stretch tensor, and which satisfies strong ellipticity for the entire range of deformation. By acknowledging these difficulties associated with such construction and the fact that the loss of ellipticity is not a mathematical pathology, we use the nine inequalities associated with any incompressible and isotropic hyperelastic material established by Zubov and Rudev (2011) to determine the domain where the ellipticity conditions are satisfied for the derived Hencky strain based stored energy function. We also show that the constitutive relation obtained from the derived potential satisfies Hill inequalities (or it is Hill-stable), and that the Cauchy stress is a monotone increasing function of Hencky strain in plane stress conditions. Apart from implying B-E inequalities, strong ellipticity also implies separate convexity or tension-extension inequalities.

Hill (1970) proposed a one-parameter family of constitutive inequalities involving Jaumann derivative of the Kirchhoff stress and symmetric part of velocity gradient for isotropic elastic solids, which in turn implies a second family of inequalities concerning time derivatives of Seth-Hill strain, parametrized with the same parameter m, and its corresponding conjugate stress (also see proposition 18.6.5 of Silhavy, 2013). On the suitability of this inequality, Silhavy (2013) remarks in chapter 18 of his book that *This does not seem to contradict any theoretical or experimental evidence.* When the parameter $m = 1/2$, Hill showed that Coleman-Noll inequality follows from Hill inequality, which in turn implies O-F inequality. Recall that (Rivlin, 2004) refuted the suitability of O-F inequality for nearly incompressible and incompressible elastic materials. Interestingly, only when the parameter m is zero, i.e., for Hencky strain and its conjugate Kirchhoff stress, is the Baker-Ericksen condition satisfied. Further, for the incompressible counterpart, only hyperelastic formulations based on Hencky strain is compatible with Hill's inequality. We show in Section 3.4 that the derived potential is Hill stable.

In this paper, we propose a constitutive equation for human brain tissue based on Lode invariants of Hencky strain tensor. By taking a cue from a global universal relation for incompressible isotropic elastic solid (see Monigari and Kannan, 2013; Wineman and Gandhi, 1984), the independence of total normal force and torque associated with twisting a cylindrical specimen requires that the potential be a function of both the invariants. Accordingly, assuming that the brain tissue is incompressible, we seek to determine the mathematical structure of the potential based on the invariants that measure the magnitude of distortion K_2 and the mode of distortion K_3. The former invariant quantifies the extent of distortion in a neutral manner irrespective of the type of distortion such as uniaxial, equibiaxial and pure shear, whereas the latter remains unchanged for any magnitude of a particular type of distortion (see Chen et al., 2012; Criscione et al., 2000). In

other words, a change in the latter is connected with the change of type of distortion. As an additional benefit, the most general representation of Cauchy stress involves a unit tensor basis $\mathbf{N}_0$, $\mathbf{N}_1$ and $\mathbf{N}_2$ that are mutually orthogonal to each other together with the first and the second response functions as coefficients of $\mathbf{N}_1$ and $\mathbf{N}_2$, respectively. By exploiting the physical meaning of the invariants and the orthogonality of unit tensor basis, we delineate a procedure for constructing a potential that is a function of both the invariants: (1) Only the first response function γ_1 is involved in simple tension and compression. Concomitantly, experimental evidence suggests an exponential function of K_2 with $\mathrm{K}_3 = \pi/6$ for tension and $-\pi/6$ for compression (2) The shear modulus parameter in γ_1 is assumed to be a function of K_3.[2] Consequently, the first response function is a function of K_2 and K_3. (3) The response function γ_1 is integrated to obtain the stored energy or the elastic potential. For small deformations, the stored energy must only be a quadratic function of K_2 for consilience with that of linearized elasticity. Accordingly, the stored energy is corrected by removing the mode-dependence appearing as the coefficient of K_2^2 and the corrected response functions are obtained as a function of K_2 and K_3. (4) For the constitutive equation to admit a uniaxial response, the second response function γ_2 must vanish at $\mathrm{K}_3 = \pm\pi/6$. (5) A priori analysis using Baker-Ericksen inequalities[3] is used to determine the mathematical form of the shear modulus function and corrected in order for the derivative to vanish at $\mathrm{K}_3 = \pm\pi/6$. (6) The modulus function is further corrected to satisfy the requirement of the stronger Hill inequality. (7) For any potential satisfying Hill inequality, true-stress-true-strain monotonicity for plane stress conditions is shown to hold.

We refer the readers to the papers on constitutive modelling of brain tissue (see Goriely et al., 2015; de Rooij and Kuhl, 2016), biological tissues in general (see Chagnon et al., 2015; Humphrey, 2003; Mihai and Goriely, 2017; Wex et al., 2015) and elastomers (see Boyce and Arruda, 2000; Marckmann and Verron, 2006; Mihai and Goriely, 2017), and the references therein for a comprehensive review of various constitutive equations that have been proposed. To the best of our knowledge, amongst the proposed constitutive equations for isotropic and hyperelastic materials, this is the first paper to partially condense the mathematical structure of the potential in terms of the Lode invariants from *a priori* analysis using Baker-Ericksen inequalities. When both the invariants are involved in the construction of the potential, where the invariant K_3 appears in the exponential function through the shear modulus (see Eq. (47)), *a priori* analysis is essential to obtain the correct functional form of the shear modulus. Otherwise, the derived constitutive equation is very likely to violate the B-E inequalities during some deformation. Compared to the predictions of the constitutive equation proposed by Mihai et al. (2017) for brain tissue, our model emulates the mechanical behavior qualitatively and quantitatively better with the same number of material parameters.

2. Shear superposed on uniaxial deformation

The combined loading experiments on human brain tissue performed by Budday et al. (2017) uses the motion studied by Wineman and Gandhi (1984) for obtaining universal relations. Such experiments are suitable for obtaining constitutive equations that depend on the magnitude and the mode of distortion because the material is subjected to different modes of distortion. The pertinent motion for an incompressible material is given through:

$$\mathrm{x} = \frac{1}{\sqrt{\lambda}}\,\mathrm{X} + \lambda\gamma\,\mathrm{Z}, \tag{1a}$$

$$\mathrm{y} = \frac{1}{\sqrt{\lambda}}\,\mathrm{Y}, \tag{1b}$$

and

$$\mathrm{z} = \lambda\,\mathrm{Z}, \tag{1c}$$

where (X, Y, Z) and (x, y, z) are the coordinates of a particle in the reference and the current configuration, respectively.

The corresponding deformation gradient is given through

$$\mathbf{F} = \begin{bmatrix} \frac{1}{\sqrt{\lambda}} & 0 & \lambda\gamma \\ 0 & \frac{1}{\sqrt{\lambda}} & 0 \\ 0 & 0 & \lambda \end{bmatrix}. \tag{2}$$

Notice that the motion is isochoric since an incompressible material can only undergo isochoric motion.

The eigenvalues of the square root of left Cauchy-Green stretch tensor $\mathbf{B}$, i.e., $\mathbf{V}$, corresponding to the motion (1) are

$$\lambda_{1\mathrm{v}} = \frac{1}{\sqrt{\lambda}}, \tag{3a}$$

$$\lambda_{2\mathrm{v}} = \frac{\sqrt{\left(\gamma^2+1\right)\lambda^2 - \frac{\sqrt{\left(\gamma^2+1\right)^2\lambda^5 + 2\left(\gamma^2-1\right)\lambda^2 + \frac{1}{\lambda}}}{\sqrt{\lambda}} + \frac{1}{\lambda}}}{\sqrt{2}}, \tag{3b}$$

[2] Data presented in Mihai et al. (2015) suggests that shear modulus of brain tissue must be a function of the mode of distortion.

[3] One expects a constitutive equation to at least satisfying B-E inequalities.

and

$$\lambda_{3v} = \frac{\sqrt{\left(\gamma^2+1\right)\lambda^2 + \frac{\sqrt{\left(\gamma^2+1\right)^2\lambda^5 + 2\left(\gamma^2-1\right)\lambda^2 + \frac{1}{\lambda}}}{\sqrt{\lambda}} + \frac{1}{\lambda}}}{\sqrt{2}}. \tag{3c}$$

Lode invariants are given through (see Chen et al., 2012; Criscione et al., 2000)

$$K_1 = \frac{1}{\sqrt{3}}\mathrm{tr}(\ln\mathbf{V}), \tag{4a}$$

$$K_2 = ||\mathrm{dev}(\ln\mathbf{V})||, \tag{4b}$$

and

$$K_3 = \frac{1}{3}\sin^{-1}\left(\frac{\sqrt{6}\ \mathrm{tr}((\mathrm{dev}(\ln\mathbf{V}))^3)}{||\mathrm{dev}(\ln\mathbf{V})||^3}\right), \tag{4c}$$

where K_1, K_2 and K_3 measure the extent of dilation or contraction, magnitude of distortion and the mode of distortion, respectively. By substituting Eq. (3) in Eq. (4), for an incompressible material one arrives at the following three equations:

$$K_1 = 0, \tag{5a}$$

$$K_2 = \frac{1}{2}\sqrt{2\coth^{-1}\left(\frac{\left(\gamma^2+1\right)\lambda^3+1}{\sqrt{\left(\gamma^2+1\right)^2\lambda^6 + 2\left(\gamma^2-1\right)\lambda^3+1}}\right)^2 + \frac{3(\ln(\lambda))^2}{2}} \tag{5b}$$

and

$$K_3 = \frac{1}{3}\sin^{-1}\left(\frac{3\sqrt{\frac{3}{2}}\left(2I_2^2\ln(\lambda) - (\ln(\lambda))^3\right)}{4K_2^3}\right). \tag{5c}$$

One can solve for $\ln(\lambda)$ in Eq. (5c) in terms of the other invariants. The cubic equation has a positive discriminant, and hence, all the solutions are real. Out of the three real roots, only one of the solutions changes sign as required by the expression for $\ln(\lambda)$. Moreover, corresponding to each of the expressions that do not change sign, the solution for γ is a pair of complex conjugates. Accordingly, the appropriate solutions for the parameters λ and γ are expressed as

$$\lambda = e^{2\sqrt{\frac{2}{3}}K_2\sin(K_3)} \tag{6a}$$

and

$$\gamma = \pm\sqrt{-e^{-2\sqrt{6}K_2\sin(K_3)} + 2e^{-\sqrt{6}K_2\sin(K_3)}\cosh\left(\sqrt{2}K_2\cos(K_3)\right) - 1}, \tag{6b}$$

i.e., one can shear along the positive or negative X direction.

For incompressible and isotropic hyperelastic materials, $\tilde{W}(\ln\mathbf{V})$ becomes $W(K_2, K_3)$, where the invariants K_2 and K_3 are expressed through Eqs. (4b) and (4c), and Cauchy stress is represented through an orthonormal tensor basis $\mathbf{N}_0, \mathbf{N}_1$ and $\mathbf{N}_2$ (see Chen et al., 2012):

$$\mathbf{T} = -p\mathbf{N}_0 + \frac{\partial W}{\partial K_2}\mathbf{N}_1 + \frac{1}{K_2}\frac{\partial W}{\partial K_3}\mathbf{N}_2, \tag{7}$$

where $\mathrm{tr}(\mathbf{N}_i\mathbf{N}_j) = 0\ (i \neq j)$ and $\mathrm{tr}(\mathbf{N}_i\mathbf{N}_i) = 1$ (no sum on the index i), $i = 0, 1, 2$. The Lagrange multiplier, the first and the second response functions are p, $\gamma_1(K_2, K_3) = \frac{\partial W}{\partial K_2} = \mathbf{T}\cdot\mathbf{N}_1$ and $\gamma_2(K_2, K_3) = \frac{1}{K_2}\frac{\partial W}{\partial K_3} = \mathbf{T}\cdot\mathbf{N}_2$, respectively. In terms of the tensor $\mathbf{V}$, mutually orthogonal unit tensors are defined through

$$\mathbf{N}_0 = \frac{\partial K_1}{\partial \ln\mathbf{V}} = \frac{\mathbf{I}}{\sqrt{3}}, \tag{8a}$$

$$\mathbf{N_1} = \frac{\partial K_2}{\partial \ln\mathbf{V}} = \frac{\mathrm{dev}(\ln\mathbf{V})}{K_2} \tag{8b}$$

and

$$\mathbf{N}_2 = K_2\frac{\partial K_3}{\partial \ln\mathbf{V}} = \frac{\sqrt{6}}{\cos(3K_3)}\left(\mathbf{N}_1^2 - \frac{1}{3}\mathbf{I} - \mathrm{tr}(\mathbf{N}_1^3)\mathbf{N}_1\right), \tag{8c}$$

where $\mathbf{I}$ is the identity tensor. After performing all the operations described in Eqs. (7) and (8), $\mathrm{tr}(\ln\mathbf{V})$ is set to zero *a posteriori* in the same equations for incompressible materials.

On using Eqs. (6) and (8b), assuming positive γ, immediately one can calculate the components of the tensor basis for the motion (1) in terms of the invariants K_2 and K_3 :

$$N_{1xx} = \frac{3\cos(K_3)\left(\cosh\left(\sqrt{2}K_2\cos(K_3)\right) - e^{\sqrt{6}K_2\sin(K_3)}\right)\operatorname{csch}\left(\sqrt{2}K_2\cos(K_3)\right) + \sin(K_3)\sqrt{3}}{3\sqrt{2}}, \tag{9a}$$

$$N_{1xy} = 0, \tag{9b}$$

$$N_{1xz} = \frac{\cos(K_3)\sqrt{-e^{2\sqrt{6}K_2\sin(K_3)} + 2e^{\sqrt{6}K_2\sin(K_3)}\cosh\left(\sqrt{2}K_2\cos(K_3)\right) - 1}}{\sqrt{\cosh\left(2\sqrt{2}K_2\cos(K_3)\right) - 1}}, \tag{9c}$$

$$N_{1yy} = -\sqrt{\frac{2}{3}}\sin(K_3), \tag{9d}$$

$$N_{1yz} = 0, \tag{9e}$$

and

$$N_{1zz} = \frac{3\cos(K_3)\left(e^{\sqrt{6}K_2\sin(K_3)} - \cosh\left(\sqrt{2}K_2\cos(K_3)\right)\right)\operatorname{csch}\left(\sqrt{2}K_2\cos(K_3)\right) + \sin(K_3)\sqrt{3}}{3\sqrt{2}}. \tag{9f}$$

The components of $\mathbf{N}_2$ are readily obtained using Eq. (8c):

$$N_{2xx} = \frac{3\sin(K_3)\operatorname{csch}\left(\sqrt{2}K_2\cos(K_3)\right)\left(e^{\sqrt{6}K_2\sin(K_3)} - \cosh\left(\sqrt{2}K_2\cos(K_3)\right)\right) + \sqrt{3}\cos(K_3)}{3\sqrt{2}}, \tag{10a}$$

$$N_{2xy} = 0, \tag{10b}$$

$$N_{2xz} = -\frac{\sin(K_3)\sqrt{-e^{2\sqrt{6}K_2\sin(K_3)} + 2e^{\sqrt{6}K_2\sin(K_3)}\cosh\left(\sqrt{2}K_2\cos(K_3)\right) - 1}}{\sqrt{\cosh\left(2\sqrt{2}K_2\cos(K_3)\right) - 1}}, \tag{10c}$$

$$N_{2yy} = -\sqrt{\frac{2}{3}}\cos(K_3), \tag{10d}$$

$$N_{2yz} = 0 \tag{10e}$$

and

$$N_{2zz} = \frac{3\sin(K_3)\operatorname{csch}\left(\sqrt{2}K_2\cos(K_3)\right)\left(\cosh\left(\sqrt{2}K_2\cos(K_3)\right) - e^{\sqrt{6}K_2\sin(K_3)}\right) + \sqrt{3}\cos(K_3)}{3\sqrt{2}}. \tag{10f}$$

For the Eqs. (9) and (10), K_2 and K_3 are expressed through the Eqs. (4b) and (4c), respectively, with $\operatorname{tr}(\ln\mathbf{V})$ being set to zero. A stored energy function in terms of the invariants K_2 and K_3 reduced with $\operatorname{tr}(\ln\mathbf{V}) = 0$ is sufficient to calculate Cauchy stress by using Eq. (7). Accordingly, unless stated otherwise, only the invariants in the reduced form is used from this point forward.

3. A novel procedure for the construction of a potential based on both the Lode invariants

3.1. Compatibility condition for the second response function

By employing a limiting process $K_3 \to \pm\frac{\pi}{6}$ to the Eqs. (9) and (10), one can obtain the components of $\mathbf{N}_1$ and $\mathbf{N}_2$ corresponding to uniaxial tension and compression along the z-direction, respectively:

$$\mathbf{N}_1 = \begin{bmatrix} \mp\frac{1}{\sqrt{6}} & 0 & 0 \\ 0 & \mp\frac{1}{\sqrt{6}} & 0 \\ 0 & 0 & \pm\sqrt{\frac{2}{3}} \end{bmatrix} \tag{11a}$$

and

$$\mathbf{N}_2 = \begin{bmatrix} \frac{1}{\sqrt{2}} & 0 & 0 \\ 0 & -\frac{1}{\sqrt{2}} & 0 \\ 0 & 0 & 0 \end{bmatrix}. \tag{11b}$$

On substituting Eq. (11) in Eq. (7), two different expressions are obtained for each of the lateral stresses that are non-zero for loading along the z-direction, which is unrealistic if $\gamma_2 \neq 0$. By using a universal relation for uniaxial deformation (tension or compression), i.e., all the components of stress are zero except along the loading direction and the orthogonality of unit tensor basis, $\mathbf{T} \cdot \mathbf{N}_2 = \gamma_2 = 0$. In other words, compatibility with the said universal relation demands that the second response function γ_2 must vanish for $\mathrm{K}_3 = \pm\frac{\pi}{6}$.

3.2. The mathematical form of the first response function is based on uniaxial data

For uniaxial tension and compression along the z-direction, since $\gamma_2 = 0$, the Lagrange multiplier is determined to be $p = \mp\frac{\gamma_1}{\sqrt{6}}$ by using the traction-free condition on the lateral faces on using the Eqs. (11a) and (7). Accordingly, the longitudinal stress $\mathrm{T}_{33} = \pm\gamma_1\left(\frac{1}{\sqrt{6}} + \sqrt{\frac{2}{3}}\right)$, i.e., only the first response function is involved in the expression for uniaxial stress. Consequently, the measured uniaxial tensile or compressive stress T_{33} for corona-radiata of the human brain tissue favors the following form for γ_1:

$$\gamma_1 = \mathrm{a}\left(\mathrm{e}^{\mathrm{K}_2\mathrm{b}(\mathrm{K}_3)} - 1\right), \tag{12}$$

where a is a positive scaling parameter for γ_1 and the mathematical form of $b(\mathrm{K}_3)$ will be determined by *a priori* analysis of B-E inequalities in Section 3.3. The function 'b' plays the role of a modulus parameter (and therefore value of the function is positive) dependent on the mode of deformation, and hence can assume different moduli in tension and compression akin to that observed in experiments. Notice that for a body in undeformed state, the first response function assumes the value zero whenever $\mathrm{K}_2 = 0$. One can obtain the potential function W by integrating γ_1 with respect to K_2, i.e.,

$$\begin{aligned} \mathrm{W} &= \int \gamma_1 \mathrm{d}\mathrm{K}_2 \\ &= \mathrm{a}\left(\frac{\mathrm{e}^{\mathrm{K}_2\mathrm{b}(\mathrm{K}_3)}}{\mathrm{b}(\mathrm{K}_3)} - \mathrm{K}_2\right) + \mathrm{g}(\mathrm{K}_3), \end{aligned} \tag{13}$$

where $\mathrm{g}(\mathrm{K}_3)$ is determined to be,

$$\mathrm{g}(\mathrm{K}_3) = -\frac{\mathrm{a}}{\mathrm{b}(\mathrm{K}_3)}. \tag{14}$$

on using the stipulation that $\mathrm{W} = 0$ whenever $\mathrm{K}_2 = 0$. The power series expansion of the Eq. (13) reduces to $(a/2)\mathrm{K}_2{}^2\mathrm{b}(\mathrm{K}_3) + \mathrm{O}(\mathrm{K}_2{}^3)$, and upon linearization the leading term becomes $(a/2)\mathrm{tr}(\boldsymbol{\epsilon}^2)b(\mathrm{K}_3)$, i.e., it is dependent on the mode of distortion. For consilience with that of linearized elasticity, Eq. (13) is corrected by removing the dependence on the mode of distortion and adding a quadratic term only involving K_2:

$$\mathrm{W} = -\frac{1}{2}\mathrm{a}\mathrm{K}_2{}^2\mathrm{b}(\mathrm{K}_3) + \frac{\mathrm{a}\mathrm{e}^{\mathrm{K}_2\mathrm{b}(\mathrm{K}_3)}}{\mathrm{b}(\mathrm{K}_3)} - \mathrm{a}\mathrm{K}_2 + \frac{\mathrm{c}\mathrm{K}_2{}^2}{2} - \frac{\mathrm{a}}{\mathrm{b}(\mathrm{K}_3)}. \tag{15}$$

Thereupon, the series approximation of the corrected W becomes

$$\mathrm{W} = \frac{\mathrm{c}\mathrm{K}_2{}^2}{2} + \frac{1}{6}\mathrm{a}\mathrm{K}_2{}^3\mathrm{b}(\mathrm{K}_3)^2 + \mathrm{O}\left(\mathrm{K}_2{}^4\right), \tag{16}$$

where c is shear modulus that characterizes small deformation and the dependence on K_3 is shifted to the cubic term. Eq. (15) is the correct general form of the potential, which will be invoked to determine the final form of the potential after the function $\mathrm{b}(\mathrm{K}_3)$ is derived. In a related work, Sendova and Walton (2005) showed that for special motions of materials for which the stored energy W is a function of K_2, W must at least grow exponentially with K_2 to satisfy the requirement of strong ellipticity. Subsequently, the corrected first response function γ_1 becomes

$$\gamma_1 = \mathrm{a}\left(\mathrm{e}^{\mathrm{K}_2\mathrm{b}(\mathrm{K}_3)} - 1\right) - \mathrm{a}\mathrm{K}_2\mathrm{b}(\mathrm{K}_3) + \mathrm{c}\mathrm{K}_2 \tag{17}$$

and the second response functions γ_2 is calculated to be

$$\begin{aligned} \gamma_2 &= \frac{1}{\mathrm{K}_2}\frac{\partial \mathrm{W}}{\partial \mathrm{K}_3} \\ &= -\frac{a\left(\mathrm{K}_2{}^2\mathrm{b}(\mathrm{K}_3)^2 - 2\mathrm{K}_2\mathrm{b}(\mathrm{K}_3)\mathrm{e}^{\mathrm{K}_2\mathrm{b}(\mathrm{K}_3)} + 2\mathrm{e}^{\mathrm{K}_2\mathrm{b}(\mathrm{K}_3)} - 2\right)\mathrm{b}'(\mathrm{K}_3)}{2\mathrm{K}_2\mathrm{b}(\mathrm{K}_3)^2}. \end{aligned} \tag{18}$$

Experimental data for brain tissue (see Mihai and Goriely, 2017) suggests that shear modulus in compression is more than that in tension. Therefore, it reasonable to assume that $\mathrm{b}'(\mathrm{K}_3) < 0$, and consequently it is easy to show that $\gamma_2 < 0$.

3.3. A priori analysis using Baker-Ericksen inequalities

Apart from frame indifference, material symmetry and compatibility of the second response function, a constitutive equation has to satisfy constitutive inequalities which are known to produce reasonable physical response. One such inequality is the weakly restrictive Baker-Ericksen conditions. Without loss of generality, let λ_1, λ_2 and $1/\lambda_1\lambda_2$ be the eigenvalues of $\mathbf{V}$. Consequently, the Lode invariants are given through

$$K_2 = \sqrt{2}\sqrt{\ln(\lambda_1)\ln(\lambda_2) + \ln^2(\lambda_1) + \ln^2(\lambda_2)} \tag{19a}$$

and

$$K_3 = -\frac{1}{3}\sin^{-1}\left(\frac{3\sqrt{6}\ln(\lambda_1)\ln(\lambda_2)(\ln(\lambda_1)+\ln(\lambda_2))}{{K_2}^3}\right). \tag{19b}$$

Baker-Ericksen inequalities are expressed as

$$\big(t_i - t_j\big)\big(\ln(\lambda_i) - \ln(\lambda_j)\big) \geq 0, \;\; i,j = 1,2,3, \tag{20}$$

where t_i are eigenvalues of Cauchy stress, and the equality holds whenever $\lambda_i = \lambda_j$. By substituting the eigenvalues of $\mathbf{V}$ in the constitutive relation (7), one can obtain the eigenvalues of Cauchy stress in terms of the eigenvalues of $\mathbf{V}$. Consequently, the eigenvalues of Cauchy stress are substituted in the left hand side of (20) and the expression $(\ln(\lambda_i) - \ln(\lambda_j))^2$ is factored. The remaining expressions in the left hand side of the product (20) are the following three inequalities:

$$1 + \frac{\gamma_2}{\gamma_1}\left(\frac{\sec(3K_3)\big(\sqrt{6}(\ln(\lambda_1)+\ln(\lambda_2)) - K_2\sin(3K_3)\big)}{K_2}\right) > 0, \tag{21a}$$

$$1 + \frac{\gamma_2}{\gamma_1}\left(-\frac{\sec(3K_3)\big(K_2\sin(3K_3) + \sqrt{6}\ln(\lambda_1)\big)}{K_2}\right) > 0 \tag{21b}$$

and

$$1 + \frac{\gamma_2}{\gamma_1}\left(-\frac{K_2\tan(3K_3) + \sqrt{6}\sec(3K_3)\ln(\lambda_2)}{K_2}\right) > 0, \tag{21c}$$

where $\gamma_1 = \partial W/\partial K_2$ and $\gamma_2 = (1/K_2)\partial W/\partial K_3$. Therefore, the above three inequalities must strictly be satisfied even if $\ln(\lambda_i) = \ln(\lambda_j)$. On substituting the expressions for $\ln(\lambda_1)$ and $\ln(\lambda_2)$ in terms of the Lode invariants (derived in Appendix A) in Eq. (21), the coefficient of γ_2/γ_1 becomes independent of K_2, and each left hand side of the above inequalities results in the three inequalities expressed below:

$$1 + \frac{\gamma_2}{\gamma_1}\cot(K_3 + \frac{\pi}{6}) > 0, \tag{22a}$$

$$1 + \frac{\gamma_2}{\gamma_1}(-\tan(K_3)) > 0 \tag{22b}$$

and

$$1 + \frac{\gamma_2}{\gamma_1}\cot(K_3 - \frac{\pi}{6}) > 0. \tag{22c}$$

In other words, inequalities (22) are equivalent to that of (21) for any $W(K_2, K_3)$. Notice that the B-E inequalities in Eq. (22) are completely expressed in terms of the invariants. As discussed in Section 3.2, for a given K_3, $\gamma_2/\gamma_1 < 0$, and the worst case amongst the inequalities (22) is realized when $|\gamma_2/\gamma_1|$ takes the maximum possible value when considered along with the largest positive coefficient. Accordingly, if the inequality (22a) is satisfied, then the other two are automatically satisfied. In order to determine the nature of γ_2/γ_1, the numerator of the derivative of γ_2/γ_1 with respect to K_2 is expressed in the form of series[4]:

$$\begin{aligned}\frac{\partial(\frac{\gamma_2}{\gamma_1})}{\partial K_2} = \sum_{n=4}^{\infty}\frac{ab'(K_3)}{2K_2^2 b(K_3)^2\gamma_1^2}\Bigg(c\Bigg(-\frac{4}{(n-2)!} + \frac{4}{(n-1)!} + \frac{2}{(n-3)!}\Bigg)K_2{}^n b(K_3)^{n-1} \\ + a\Bigg(\Bigg(\frac{1}{(n-2)!} - \frac{1}{(n-3)!}\Bigg)n! - 4(n+1) + 2^{n+1}\Bigg)\frac{(K_2 b(K_3))^n}{n!}\Bigg).\end{aligned} \tag{23}$$

Since $b'(K_3)$ is assumed to be negative together with the fact that each term of Eq. (23) is negative, implies that γ_2/γ_1 is monotone decreasing with respect to K_2. Therefore, the worst case circumstance is realized when

$$\lim_{K_2\to\infty}\frac{\gamma_2}{\gamma_1} = \frac{b'(K_3)}{b(K_3)} \tag{24}$$

[4] The series expression has an arbitrary radius of convergence.

and the inequality (22a) reduces to

$$1 + \frac{b'(K_3)}{b(K_3)} \cot(K_3 + \frac{\pi}{6}) > 0, \tag{25}$$

which is a differential inequality only involving the invariant K_3. Even though the left hand side of inequality (25) is set to zero in order to obtain the solution[5] $b_0\cos(K_3 + \frac{\pi}{6})$ with the derivative at $K_3 = -\pi/6$ being zero, a correction to this solution is necessitated by the compatibility established in Section 3.1, which in turn renders the corrected solution to strictly satisfy the above inequality. Accordingly, the derivative of $b_0\cos(K_3 + \frac{\pi}{6})$ is multiplied with a suitable exponential function with values approaching a maximum of unity at all K_3 except near $\pi/6$, and vanishes at $\pi/6$. By integrating the corrected derivative with respect to K_3, one arrives at the appropriate function 'b', i.e.,

$$b(K_3) = b_0\left(\frac{e^{\frac{1}{2}\left(b_1 - 2b_1\cos\left(K_3 + \frac{\pi}{6}\right)\right)}}{b_1} + \cos\left(K_3 + \frac{\pi}{6}\right)\right), \tag{26}$$

where 'a' is the scaling constant for W, b_0 is the constant connected with the mode-dependent modulus function $b(K_3)$, b_1 is a constant that controls the 'closeness' of the corrected function $b(K_3)$ with that of the zero solution $b_0\cos(K_3 + \frac{\pi}{6})$ and c is the only modulus that is active during small deformations. The solution (26) also satisfies the inequality (25) with the lowest value amongst the left hand side of inequalities (22) being $(b_1 + 1)/(e^{b_1/2}b_1 + 1)$, i.e., the inequalities are always strictly satisfied for any finite b_1.

The use of principal invariants or for that matter principal stretches based formulation is not readily amenable with the foregoing analysis because it results in partial differential inequalities, which are much more difficult to analyze.

3.4. Correction of modulus function $b(K_3)$ using hill inequality

Recall that if a potential based on Hencky strain is Hill-stable, then it automatically satisfies the B-E inequalities, but, generally the vice versa does not hold. The modulus function $b(K_3)$ expressed in Eq. (26) needs to be further corrected so that the Hill inequality is satisfied for all positive values of b_1. To that end, we begin by stating the Hill inequality for non-zero **D** and any Hencky strain:

$$\mathrm{tr}(\overset{\circ}{\boldsymbol{\tau}}\,\mathbf{D}) > 0, \tag{27}$$

where $\overset{\circ}{\boldsymbol{\tau}}$ is the Jaumann derivative of Kirchhoff stress. By expanding Eq. (27), one arrives at

$$\mathrm{tr}(\dot{\boldsymbol{\tau}}\mathbf{D}) + \mathrm{tr}(\boldsymbol{\tau}\mathbf{W}_1\mathbf{D}) - \mathrm{tr}(\mathbf{W}_1\boldsymbol{\tau}\mathbf{D}) > 0 \tag{28}$$

with τ being a function of $\ln(\mathbf{V})$. We show in Appendix B that $\ln(\mathbf{V})$ and **D** have the same eigenvectors and hence the above equation reduces to

$$\mathrm{tr}(\dot{\boldsymbol{\tau}}\mathbf{D}) > 0. \tag{29}$$

For incompressible materials Kirchhoff and the Cauchy stress are indistinguishable and the above equation reduces to

$$-\dot{p}\,\mathrm{tr}(\mathbf{D}) + \mathrm{tr}(\dot{\mathbf{T}}^e\mathbf{D}) = \mathrm{tr}(\dot{\mathbf{T}}^e\mathbf{D}) > 0, \tag{30}$$

where p is the Lagrange multiplier and $\mathbf{T}^e$ is the extra part of the Cauchy stress. One can show that the inequality (30) implies that the Hessian of the stored energy with respect to all the principal values of Hencky strain must be positive definite (see Appendix C). In other words, Hessian must be computed prior to the application of the incompressibility constraint (free Hessian) and the physically realizable Hessian is later obtained by applying the constraint (see Appendix C). After applying the constraint, one of the eigenvalues of the Hessian becomes null, and the Hessian reduces to a 2×2 matrix. Chen et al. (2012) showed that one can rewrite the free Hessian in terms of the derivatives involving the Lode invariants. Accordingly, for incompressible materials, necessary and sufficient conditions for the Hessian to be positive definite are obtained by applying the incompressibility constraint on the free Hessian expressed in terms of the Lode invariants, i.e, the required conditions are,

$$\frac{\partial^2 W}{\partial K_2^2} > 0 \tag{31a}$$

and

$$\left(\frac{1}{K_2^2}\frac{\partial^2 W}{\partial K_3^2} + \frac{1}{K_2}\frac{\partial W}{\partial K_2}\right)\frac{\partial^2 W}{\partial K_2^2} - \left(\frac{\partial}{\partial K_2}\left(\frac{1}{K_2}\frac{\partial W}{\partial K_3}\right)\right)^2 > 0. \tag{31b}$$

For a compressible material, if a potential W is Hill stable, in addition to automatically satisfying B-E inequalities, it automatically satisfies the weaker constitutive assumption of Kirchhoff stress-stretch-invertibility, which in turn implies that

[5] Produces the maximum change in the value of function.

the shear modulus and bulk modulus are positive for the linearized elastic material[6] (refer to Neff et al., 2015). Consequently, at small deformations one is guaranteed finite wave speeds. The first inequality (31a) implies that the first response function γ_1 must be monotone increasing with respect to the invariant K_2 (or W is partially convex with respect to K_2), which is automatically satisfied because of the choice of the function assumed for γ_1 (see Section 3.2). The second inequality (31b) expresses the diagonal dominance of the Hessian in terms of the Lode invariants. One can rewrite Eq. (31b) as,

$$\left(\frac{\partial^2 W}{\partial K_2^2}\right)^2\left(\frac{\frac{1}{K_2^2}\frac{\partial^2 W}{\partial K_3^2}+\frac{1}{K_2}\frac{\partial W}{\partial K_2}}{\frac{\partial^2 W}{\partial K_2^2}}-\left(\frac{\frac{\partial}{\partial K_2}\left(\frac{1}{K_2}\frac{\partial W}{\partial K_3}\right)}{\frac{\partial^2 W}{\partial K_2^2}}\right)^2\right)>0. \tag{32}$$

Since $(\partial^2 W/\partial K_2^2)^2$ is always positive, it immediately follows that,

$$\frac{\frac{1}{K_2^2}\frac{\partial^2 W}{\partial K_3^2}+\frac{1}{K_2}\frac{\partial W}{\partial K_2}}{\frac{\partial^2 W}{\partial K_2^2}}-\left(\frac{\frac{\partial}{\partial K_2}\left(\frac{1}{K_2}\frac{\partial W}{\partial K_3}\right)}{\frac{\partial^2 W}{\partial K_2^2}}\right)^2>0. \tag{33}$$

The series form of the corrected potential function (15) having an arbitrary radius of convergence is expressed as,

$$W=\frac{cK_2^2}{2}+\sum_{n=2}^{\infty}\frac{aK_2(K_2 b(K_3))^n}{(n+1)!}. \tag{34}$$

It is easy to show that the first term $cK_2^2/2$ satisfies Hill inequality and it suffices to show that every term in the Eq. (34) satisfies the same because the sum of positive definite Hessians calculated with respect to the principal values of $\ln \mathbf{V}$ is also positive definite. To that end, the every term in the series is substituted in Eq. (33), and the nth term can be expressed as

$$\frac{b''(K_3)}{(n+1)b(K_3)}-\frac{b'(K_3)^2}{(n+1)^2 b(K_3)^2}+\frac{1}{n}>0,\ \ n=2,3,\ldots \tag{35}$$

In other words, satisfying the above inequality for every n is sufficient to satisfy the requirement of Hill inequality if W is of the form (15). Notice that the inequality (31b) is reduced to an ordinary differential inequality involving K_3. Recall that the modulus function expressed in (26) does not satisfy the Hill inequality for all b_1. In order to mitigate this weakness, the following inequalities are considered:

$$\frac{\tilde{b}''(K_3)}{\tilde{b}(K_3)}\le\frac{\hat{b}''(K_3)}{\hat{b}(K_3)} \tag{36a}$$

and

$$\frac{\tilde{b}'(K_3)^2}{\tilde{b}(K_3)^2}\ge\frac{\hat{b}'(K_3)^2}{\hat{b}(K_3)^2}, \tag{36b}$$

where

$$\hat{b}(K_3)=b_0\left(\frac{e^{\frac{1}{2}\left(b_1-2b_1\cos\left(K_3+\frac{\pi}{6}\right)\right)}}{b_1}+\cos\left(K_3+\frac{\pi}{6}\right)+C_3\right) \tag{37a}$$

and

$$\tilde{b}(K_3)=b_0\left(\cos\left(K_3+\frac{\pi}{6}\right)+C_3\right), \tag{37b}$$

with C_3 being a positive constant. This constant will be determined such that the Hill inequality is satisfied for all b_1. This constant must be as small as possible in order for the modulus function to have the greatest change in value. Referring to the inequalities (36), the equality holds whenever $b_1\to\infty$ except at $K_3=\pi/6$. Since $\tilde{b}''(K_3)<0$, substituting Eq. (37b) in place of the function $b(K_3)$ in (35) yields a safer inequality with the left hand side (residual) b_{res} being

$$b_{res}=\frac{(n+1)\left(C_3+\cos\left(K_3+\frac{\pi}{6}\right)\right)\left(C_3 n+C_3+\cos\left(K_3+\frac{\pi}{6}\right)\right)-n\sin^2\left(K_3+\frac{\pi}{6}\right)}{n(n+1)^2\left(C_3+\cos\left(K_3+\frac{\pi}{6}\right)\right)^2}. \tag{38}$$

The value of the residual and its first derivative at $K_3=-\pi/6$ is always positive for all n, i.e.,

$$b_{res}\Big|_{K_3=-\frac{\pi}{6}}=\frac{C_3 n+C_3+1}{(C_3+1)n(n+1)}>0, \tag{39}$$

and zero, respectively. The second derivative of the residual expressed as

$$\frac{\partial b_{res}^2}{\partial K_3^2}\Big|_{K_3=-\frac{\pi}{6}}=\frac{C_3 n+C_3-2}{(C_3+1)^2(n+1)^2} \tag{40}$$

[6] If an elastic material is incompressible, on linearization, one obtains positive shear modulus and infinite bulk modulus.

implying that $K_3 = -\pi/6$ is a local maxima if $C_3 < 2/(n+1)$, and a minima otherwise. If the constant $C_3 < 2/(n+1)$, then the residual is a monotone decreasing function of K_3 with a unique maxima at $-\pi/6$, and the lowest value of the residual occurs at $K_3 = \pi/6$. There is exactly one more extrema between $-\pi/6$ and $\pi/6$ at

$$K_3 = \frac{1}{6}\left(-\pi + 6\left(\cos^{-1}\left(\frac{C_3^2(-n) - C_3^2 + 2}{C_3(n-1)}\right)\right)\right) \tag{41}$$

provided that

$$\frac{2}{n+1} \leq C_3 \leq \frac{\sqrt{n^2+30n+33} - n + 1}{4n+4}. \tag{42}$$

In such a case, it immediately implies that the extrema is a maxima because of the presence of a minima at $-\pi/6$. Then, the possibility of the residual being the largest negative number can only occur at $\pi/6$. If $C_3 > (\sqrt{n^2+30n+33} - n + 1)/(4n+4)$, then the residual is always positive. In summary, by making the residual non-negative at $K_3 = \pi/6$ is necessary to satisfy the inequality (35), which is expressed as

$$b_{res}\Big|_{K_3=\frac{\pi}{6}} = \frac{\left(C_3+\frac{1}{2}\right)(n+1)\left(C_3 n + C_3 + \frac{1}{2}\right) - \frac{3n}{4}}{\left(C_3+\frac{1}{2}\right)^2 n(n+1)^2}. \tag{43}$$

By setting the above equation to zero and solving for C_3, one arrives at

$$C_3 = -\frac{2 + n - \sqrt{n+12}\sqrt{n}}{4n+4}, \tag{44}$$

which is always positive and monotone decreasing with respect to n. The value of C_3 corresponding to the least value of $n = 2$ satisfies the inequality (35) for all n, i.e.,

$$C_3 = \frac{\sqrt{7}-2}{6} \tag{45}$$

because $\hat{b}(K_3) \geq \tilde{b}(K_3)$ and the equality holds only when $b_1 \to \infty$ and $K_3 \neq \pi/6$. In other words, for all finite values of b_1 the inequality (35) is strictly satisfied. At $K_3 = \pi/6$, the residual is always positive. Therefore the corrected form of the Eq. (26) is expressed in the final form as

$$\hat{b}(K_3) = b_0\left(\frac{e^{\frac{1}{2}\left(b_1 - 2b_1\cos\left(K_3+\frac{\pi}{6}\right)\right)}}{b_1} + \cos\left(K_3+\frac{\pi}{6}\right) + \frac{\sqrt{7}-2}{6}\right). \tag{46}$$

The derivative of the above function also vanishes at $K_3 = \pm\pi/6$ and the fact that it is Hill stable implies that the Baker-Ericksen conditions are automatically satisfied. The larger the constant b_1, the 'closer' the above function gets to $b_0(\cos(K_3 + \pi/6) + C_3)$, except at $K_3 = \pi/6$. On the other hand, for sufficiently small values of b_1, the corrected modulus function (46) approaches $b_0/b_1 + (b_0/6)\left(1+\sqrt{7}\right)$. In other words, the modulus function '$\hat{b}$' becomes independent of the invariant K_3. Therefore, the constructed potential in the final form is expressed as

$$\begin{aligned} W = &\frac{c}{2}K_2^2 + \frac{a\left(\exp\left(b_0 K_2\left(\frac{e^{\frac{b_1}{2} - b_1\cos\left(K_3+\frac{\pi}{6}\right)}}{b_1} + \cos\left(K_3+\frac{\pi}{6}\right) + \frac{1}{6}\left(\sqrt{7}-2\right)\right)\right) - 1\right)}{b_0\left(\frac{e^{\frac{b_1}{2} - b_1\cos\left(K_3+\frac{\pi}{6}\right)}}{b_1} + \cos\left(K_3+\frac{\pi}{6}\right) + \frac{1}{6}\left(\sqrt{7}-2\right)\right)} \\ &- \frac{1}{2}ab_0K_2^2\left(\frac{e^{\frac{b_1}{2} - b_1\cos\left(K_3+\frac{\pi}{6}\right)}}{b_1} + \cos\left(K_3+\frac{\pi}{6}\right) + \frac{1}{6}\left(\sqrt{7}-2\right)\right) - aK_2 \end{aligned} \tag{47}$$

by substituting Eq. (46) in Eq. (15).

Now we draw the readers attention to the proposition 5.2 in Martin et al. (2018), which states that there is no strictly monotone increasing function of K_2^2 such that the potential is rank-one convex (or equivalently strongly elliptic[7] in the case of a sufficiently smooth potential) in the entire range of deformation. When a body is subjected to uniaxial tension or compression, i.e., $K_3 = \pm\pi/6$, respectively, the potential is in fact a convex function of K_2 because of the stipulations made on the first response function as discussed in Section 3.2. Therefore, on applying this proposition the constructed potential must lose ellipticity for some finite K_2.

[7] For example, see Dacorogna (2001).

3.5. Cauchy stress is a monotone increasing function of ln(**V**) in plane stress

In this sub-section, we show that Jog-Patil's (see Jog and Patil, 2013) true-stress-true-strain monotonicity is satisfied for plane stress. In order to show that Cauchy stress is a strictly monotone increasing function of true strain for an incompressible material in plane stress, one has to show that the 2×2 matrix

$$\frac{\partial t_i}{\partial \ln\lambda_j}(\ln\lambda_1,\ln\lambda_2,-\ln\lambda_1-\ln\lambda_2)=\frac{\partial}{\partial \ln\lambda_j}\Big(-p+\frac{\partial W}{\partial \ln\lambda_i}(\ln\lambda_1,\ln\lambda_2,\ln\lambda_3)\Big|_{\ln\lambda_3=-\ln\lambda_1-\ln\lambda_2}\Big) \tag{48}$$

is positive definite with t_3 being zero. The Lagrange multiplier p in Eq. (48) is replaced by $\partial W/\partial \ln\lambda_3$, i.e.,

$$\frac{\partial t_i}{\partial \ln\lambda_j}(\ln\lambda_1,\ln\lambda_2,-\ln\lambda_1-\ln\lambda_2)=\frac{\partial}{\partial \ln\lambda_j}\Big(-\frac{\partial W}{\partial \ln\lambda_3}\Big|_{\ln\lambda_3=-\ln\lambda_1-\ln\lambda_2}+\frac{\partial W}{\partial \ln\lambda_i}\Big|_{\ln\lambda_3=-\ln\lambda_1-\ln\lambda_2}\Big). \tag{49}$$

For a general boundary value-problem, the mathematical structure of the multiplier must be known. Recall that in Section 3.4, for an incompressible material, it was shown that the free Hessian of W is positive semi-definite because one of the eigenvalues is zero. In order to show that the Cauchy stress is a strictly monotone increasing function of Hencky strain in plane stress, the following matrix must be positive definite:

$$\frac{\partial \hat{t}_i}{\partial \ln\lambda_j}=\begin{bmatrix}(W_{,11}+W_{,33}-2W_{,13})\big| & (W_{,33}+W_{,12}-W_{,13}-W_{,23})\big| \\ (W_{,33}+W_{,12}-W_{,13}-W_{,23})\big| & (W_{,22}+W_{,33}-2W_{,23})\big|\end{bmatrix}, \tag{50}$$

where $\hat{t}_i(\ln\lambda_1,\ln\lambda_2)=t_i(\ln\lambda_1,\ln\lambda_2,-\ln\lambda_1-\ln\lambda_2)$, $W_{,ij}=\partial^2 W/\partial\ln\lambda_i\partial\ln\lambda_j$ is the free Hessian and the vertical bars indicate that the application of the incompressibility constraint a posteriori. For the sake of brevity, hereafter we will refrain from using vertical bars. The necessary and sufficient conditions for the above matrix to be positive definite are

$$W_{,11}+W_{,33}-2W_{,13}>0 \tag{51a}$$

and

$$(W_{,11}+W_{,33}-2\,W_{,13})(W_{,22}+W_{,33}-2\,W_{,23})-(W_{,33}+W_{,12}-W_{,23}-W_{,13})^2>0. \tag{51b}$$

By rearranging Eq. (51b), one arrives at

$$\begin{aligned}&\big(W_{,22}W_{,33}-W_{,23}^2\big)+\big(W_{,11}W_{,33}-W_{,13}^2\big)+\big(W_{,11}W_{,22}-W_{,12}^2\big)\\&+2(W_{,13}W_{,23}-W_{,12}W_{,33})+2(W_{,12}W_{,13}-W_{,23}W_{,11})\\&+2(W_{,12}W_{,23}-W_{,13}W_{,22})>0.\end{aligned} \tag{52}$$

Let H be the free Hessian of the constructed W in terms of the eigenvalues of Hencky strain. Recall that the free Hessian has exactly one zero eigenvalue, the other two being strictly positive, i.e., the free Hessian is positive semi-definite. By picking the vector to be $(1,0,-1)$ in the expression $H_{ij}v_jv_i$, one arrives at Eq. (51a) with the strict inequality being replaced by greater than or equal to zero. Cofactor of $W_{,ij}$ is symmetric and is defined through

$$\mathrm{cof}(H)=W_{,ij}^2-I_{1H}W_{,ij}+I_{2H}\delta_{ij}, \tag{53}$$

where I_{1H} and I_{2H} are principal invariants of the matrix $W_{,ij}$. By using Eq. (53), it is easy to show that the cofactor of the matrix H is positive semi-definite with exactly two eigenvalues being zero, and is defined through

$$\mathrm{cof}(H)=\begin{bmatrix}W_{,22}W_{,33}-W_{,23}^2 & W_{,13}W_{,23}-W_{,12}W_{,33} & W_{,12}W_{,23}-W_{,13}W_{,22}\\ W_{,13}W_{,23}-W_{,12}W_{,33} & W_{,11}W_{,33}-W_{,13}^2 & W_{,12}W_{,13}-W_{,23}W_{,11}\\ W_{,12}W_{,23}-W_{,13}W_{,22} & W_{,12}W_{,13}-W_{,23}W_{,11} & W_{,11}W_{,22}-W_{,12}^2\end{bmatrix}. \tag{54}$$

By picking the vector (1,1,1) in the expression $[\mathrm{cof}(H)]_{ij}v_jv_i$, one can show that the weaker form of Eq. (52) is satisfied. Therefore, the matrix (50) is positive semi-definite, which implies that the Cauchy stress is a monotone increasing function.

4. Comparison of effectiveness of the proposed and Mihai-Ogden model

The four material parameters associated with the proposed and Mihai-Ogden model are determined by fitting the response of both the constitutive relations with the data published in Budday et al. (2017). The parameters are optimized using differential evolution algorithm available in Mathematica®. The efficacy of the proposed and Mihai-Ogden constitutive relation is assessed by separately fitting them to the three sets of data: simple shear, uniaxial tension and compression, and the combined tension/compression and shear. After obtaining the material parameters associated with each set, the predictions of both the constitutive relations with respect to the remaining components of stress in combined tension/compression and shear are compared.

One needs to redetermine the constants for Mihai-Ogden model proposed in Mihai et al. (2017) because the originally reported constants corresponding to Budday et al. (2017) data does not even satisfy B-E inequalities. Additionally, in order to ensure that the normal stress perpendicular to the direction of shear is compressive (positive Poynting effect), one needs to establish additional constraint.

4.1. Empirical inequality for Mihai-Ogden model

The potential proposed by Mihai et al. (2017) is expressed as

$$W_{MO} = \frac{C_0}{2\alpha}\left(\lambda_1^{2\alpha} + \lambda_2^{2\alpha} + \lambda_3^{2\alpha} - 3\right) + \frac{C_1}{2}\left(\lambda_1^2 + \lambda_2^2 + \lambda_3^2 - 3\right) + \frac{C_2}{2}\left(\lambda_1^{-2} + \lambda_2^{-2} + \lambda_3^{-2} - 3\right) \tag{55}$$

and its corresponding spectral representation of Cauchy stress is

$$-p(\mathbf{n}_i \otimes \mathbf{n}_i) + C_0\lambda_i^{2\alpha}(\mathbf{n}_i \otimes \mathbf{n}_i) + C_1\lambda_i^2(\mathbf{n}_i \otimes \mathbf{n}_i) - C_2\lambda_i^{-2}(\mathbf{n}_i \otimes \mathbf{n}_i), \tag{56}$$

which in the tensor form is expressed as

$$\mathbf{T} = -p\mathbf{I} + C_0\mathbf{B}^{\alpha} + C_1\mathbf{B} - C_2\mathbf{B}^{-1}, \tag{57}$$

where $\mathbf{B}^{\alpha}$ is the α^{th} power of the positive definite left Cauchy-Green stretch tensor, and the constants in (57) and its physical meaning are identical to that of the model proposed by Mihai et al. (2017).

Since it is not easy to obtain necessary or sufficient conditions that ensure positive Poynting effect in simple shear under all conditions, we propose an empirical inequality.

On specializing the above equation for simple shear using the components of $\mathbf{B}$ computed by setting $\lambda = 1$ in Eq. (2), and applying a traction-free condition for T_{yy}, one arrives at the Lagrange multiplier and normal stress T_{zz}, respectively:

$$p = -\frac{-C_0\left(\frac{1}{\lambda}\right)^{\alpha-1} - C_1 + C_2\lambda^2}{\lambda} \tag{58}$$

and

$$\begin{aligned} T_{zz} = {} & 2^{-\alpha-1}C_0\left(\left(\gamma^2 - \sqrt{\gamma^2+4}\gamma + 2\right)^{\alpha} + \left(\gamma\left(\sqrt{\gamma^2+4} + \gamma\right) + 2\right)^{\alpha} - 2^{\alpha+1}\right) - \gamma^2 C_2 \\ & + \frac{2^{-\alpha-1}\gamma C_0\left(\left(\gamma^2 - \sqrt{\gamma^2+4}\gamma + 2\right)^{\alpha} - \left(\gamma\left(\sqrt{\gamma^2+4} + \gamma\right) + 2\right)^{\alpha}\right)}{\sqrt{\gamma^2+4}}. \end{aligned} \tag{59}$$

The normal stress induced perpendicular to the direction of shear, i.e, T_{zz} must be negative to be in line with the measurements. Further, one expects the normal stress to be monotone decreasing with respect to γ, i.e., the more the parameter γ, the more the normal stress. To that end, the power series expansion of the derivative of the above equation is computed about $\gamma = 0$:

$$\frac{dT_{zz}}{d\gamma} \approx ((\alpha-1)\alpha C_0 - 2C_2)\gamma + \frac{C_0}{6}(\alpha-2)(\alpha-1)\alpha(\alpha+1)\gamma^3 + O\left(\gamma^5\right). \tag{60}$$

The exact derivative is a complex expression and it is very difficult to arrive at necessary or sufficient condition. One can ensure that the above derivative will be negative for sufficiently small γ provided that

$$((\alpha-1)\alpha C_0 - 2C_2) < 0, \tag{61}$$

which we term it as the empirical inequality.

4.2. Determination of material parameters for Mihai-Ogden model

For a combined loading of tension/compression along the z-direction and shear along the x-direction, the normal and shear stresses are given through

$$\begin{aligned} T_{zz} = {} & -C_0\lambda^{-\alpha} + C_1\lambda^2 - \frac{C_1}{\lambda} - \frac{\gamma^2 C_2\lambda^3 + C_2}{\lambda^2} + C_2\lambda \\ & + \frac{2^{-\alpha-1}C_0\left(\left(\gamma^2-1\right)\lambda^3 + \sqrt{\left(\left(\gamma^2+1\right)\lambda^3+1\right)^2 - 4\lambda^3} + 1\right)\left(\frac{\left(\gamma^2+1\right)\lambda^3 - \sqrt{\left(\left(\gamma^2+1\right)\lambda^3+1\right)^2-4\lambda^3}+1}{\lambda}\right)^{\alpha}}{\sqrt{\left(\left(\gamma^2+1\right)\lambda^3+1\right)^2 - 4\lambda^3}} \\ & + \frac{2^{-\alpha-1}C_0\left(-\gamma^2\lambda^3 + \sqrt{\left(\left(\gamma^2+1\right)\lambda^3+1\right)^2 - 4\lambda^3} + \lambda^3 - 1\right)\left(\frac{\left(\gamma^2+1\right)\lambda^3 + \sqrt{\left(\left(\gamma^2+1\right)\lambda^3+1\right)^2-4\lambda^3}+1}{\lambda}\right)^{\alpha}}{\sqrt{\left(\left(\gamma^2+1\right)\lambda^3+1\right)^2 - 4\lambda^3}}, \end{aligned} \tag{62}$$

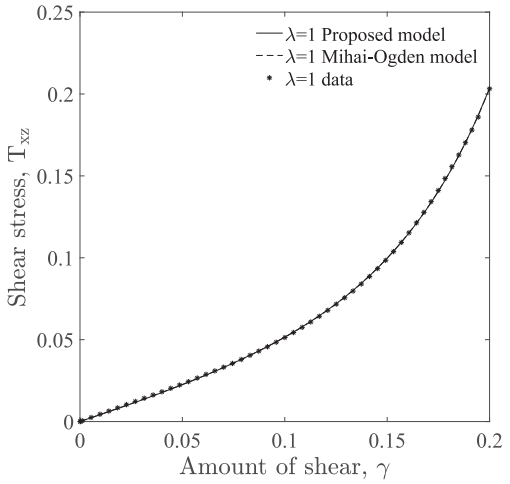

Fig. 1. Curve fitting of the predicted shear stress T_{xz} to the data for simple shear.

$$
\begin{aligned}
T_{xx} = \frac{1}{2}\Bigg(& -2C_0\lambda^{-\alpha} + 2C_1\left(\gamma^2\lambda^2 + \frac{1}{\lambda}\right) - \frac{2C_1}{\lambda} \\
& + \frac{2^{-\alpha}C_0\left(\left(\gamma^2-1\right)\lambda^3 + \sqrt{\left(\left(\gamma^2+1\right)\lambda^3+1\right)^2 - 4\lambda^3} + 1\right)\left(\frac{\left(\gamma^2+1\right)\lambda^3 + \sqrt{\left(\left(\gamma^2+1\right)\lambda^3+1\right)^2-4\lambda^3}+1}{\lambda}\right)^{\alpha}}{\sqrt{\left(\left(\gamma^2+1\right)\lambda^3+1\right)^2-4\lambda^3}} \\
& + \frac{2^{-\alpha}C_0\left(-\gamma^2\lambda^3 + \sqrt{\left(\left(\gamma^2+1\right)\lambda^3+1\right)^2 - 4\lambda^3} + \lambda^3 - 1\right)\left(\frac{\left(\gamma^2+1\right)\lambda^3 - \sqrt{\left(\left(\gamma^2+1\right)\lambda^3+1\right)^2-4\lambda^3}+1}{\lambda}\right)^{\alpha}}{\sqrt{\left(\left(\gamma^2+1\right)\lambda^3+1\right)^2-4\lambda^3}}\Bigg)
\end{aligned}
\tag{63}
$$

and

$$
\begin{aligned}
T_{xz} = & \frac{2^{-\alpha}\gamma\lambda}{\sqrt{\left(\left(\gamma^2+1\right)\lambda^3+1\right)^2-4\lambda^3}}\Bigg(2^{\alpha}\sqrt{\left(\left(\gamma^2+1\right)\lambda^3+1\right)^2-4\lambda^3}\left(C_1\lambda + C_2\right) \\
& - C_0\lambda^2\left(\frac{\gamma^2\lambda^3 - \sqrt{\left(\left(\gamma^2+1\right)\lambda^3+1\right)^2-4\lambda^3} + \lambda^3 + 1}{\lambda}\right)^{\alpha} \\
& + C_0\lambda^2\left(\frac{\gamma^2\lambda^3 + \sqrt{\left(\left(\gamma^2+1\right)\lambda^3+1\right)^2-4\lambda^3} + \lambda^3 + 1}{\lambda}\right)^{\alpha}\Bigg).
\end{aligned}
\tag{64}
$$

All the above equations in this sub-section were obtained by substituting Eq. (2) in Eq. (57) and symbolically manipulating using Mathematica®. Recall that Destrade et al. (2015) and Balbi et al. (2019) conducted simple shear experiments on porcine brain, which exhibited positive Poynting effect. The parameters associated with Mihai-Ogden model and re-

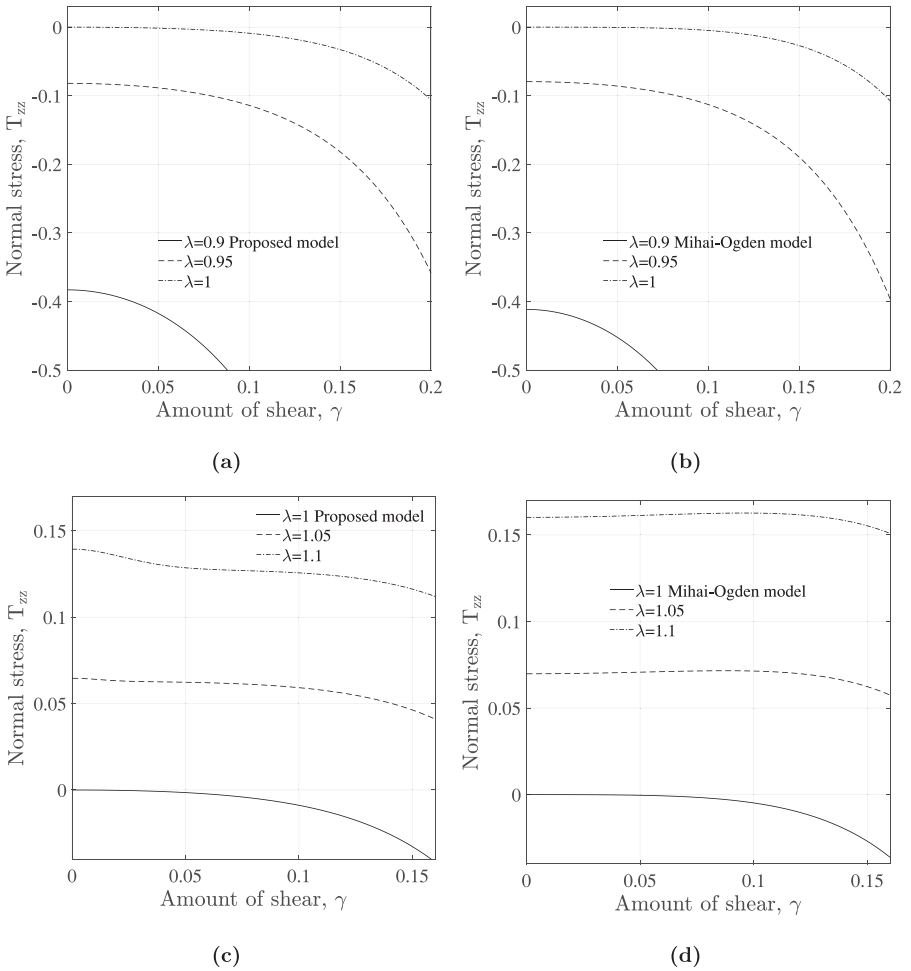

Fig. 2. Induced normal stress T_{zz} during combined loading corresponding to the material parameters obtained in Section 4.3.

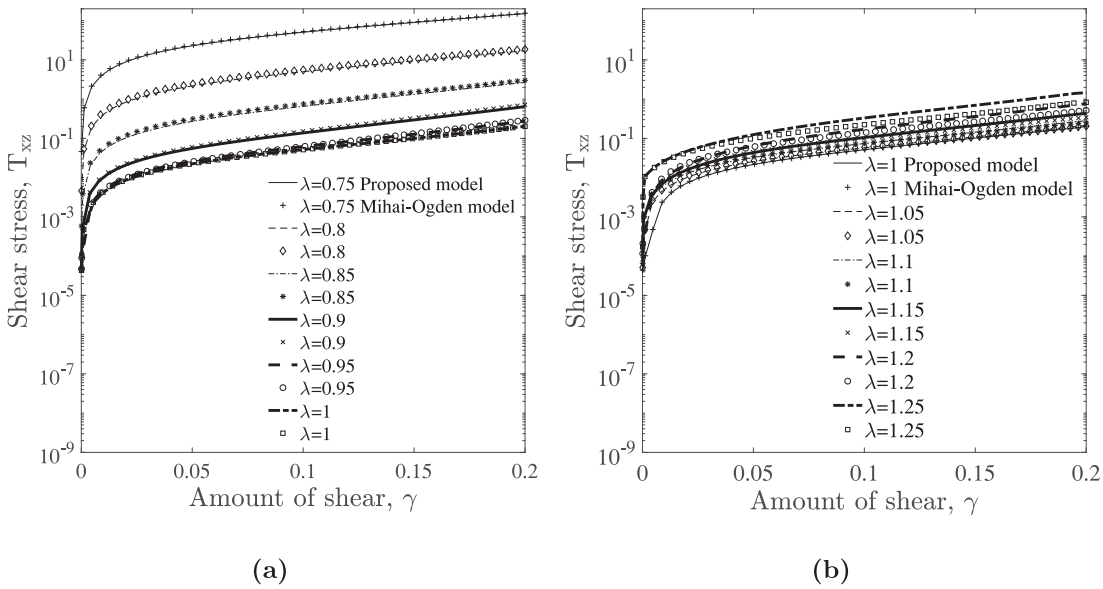

Fig. 3. Predicted shear stress T_{xz} during combined loading corresponding to material parameters obtained in Section 4.3.

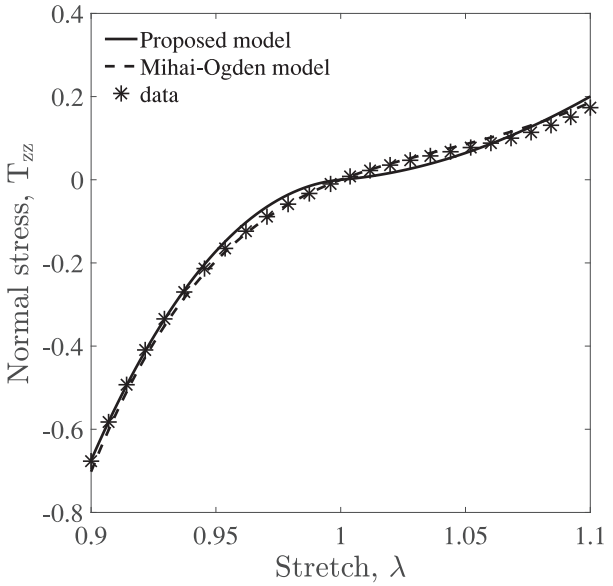

Fig. 4. The proposed and Mihai-Ogden model are fitted to uniaxial data.

Table 1
Parameters for model and Mihai-Ogden model.

	Parameters for the proposed model			
	a	b_0	b_1	c
Fitted to data for simple shear	0.00251134	31.2298	103.573[a]	0.840554
Fitted to data for uniaxial response	414.952	0.343069	2748.05	0.338293
Fitted to data for combined loading	9820.97	0.036753	19.6262	0.424742
	Parameters for Mihai-Ogden model			
	C_0	α	C_1	C_2
Fitted to data for simple shear	−0.00436129	−20.6513	1.25883	−0.91307
Fitted to data for uniaxial response	−12.2062	−2.31228	12.349	−39.81[b]
Fitted to data for combined loading	−45.4789	−1.12519	2.09917	−52.6588

[a] Constraints for Optimization are $a > 0, b_0 > 0, b_1 > 100$ and $c > 0$
[b] Adjusted to satisfy Hill inequality

ported in Mihai et al. (2017)[8] does not satisfy Baker-Ericksen inequalities and the model's prediction with those parameters produces nonphysical negative Poynting effect, i.e., the normal stress T_{zz} induced during simple shear is positive. In order to remedy the incorrectly established parameters, Mihai-Ogden model was refitted with the following conditions: $C_0\alpha > 0, C_1 > 0$ and $((\alpha - 1)\alpha C_0 - 2C_2) < 0$. These conditions also seem to ensure monotone decreasing normal stress T_{zz} during combined loading provided that the data for multiple modes of deformation are available. Ogden (1972) established sufficient conditions for the Hill inequality to be satisfied, which when applied to Mihai-Ogden model reduces to $C_0\alpha > 0, C_1 > 0$ and $C_2 > 0$. These conditions are a bit too restrictive and predicts negative Poynting when fitted to data for simple shear. Therefore, only the first two inequalities of Ogden's sufficient conditions are enforced along with the empirical inequality, and the Hill inequality is checked *a posteriori*. If the Hill inequality is violated, the parameter C_2 is adjusted in a least possible manner such that Hill condition is satisfied for a reasonably wide range of conditions. The four parameters associated with Mihai-Ogden model are determined using differential evolution algorithm with the three constraints $C_0\alpha > 0, C_1 > 0$ and $((\alpha - 1)\alpha C_0 - 2C_2) < 0$ along with the pertinent Eqs. (62) through (64) for the three sets of data discussed earlier, i.e., simple shear, uniaxial tension and compression, and combined tension/compression and shear. The resulting material parameters are listed in Table 1.

[8] $C_0 = 0.0653, \alpha = 7.1813, C_1 = -3.8201, C_2 = 3.5376$.

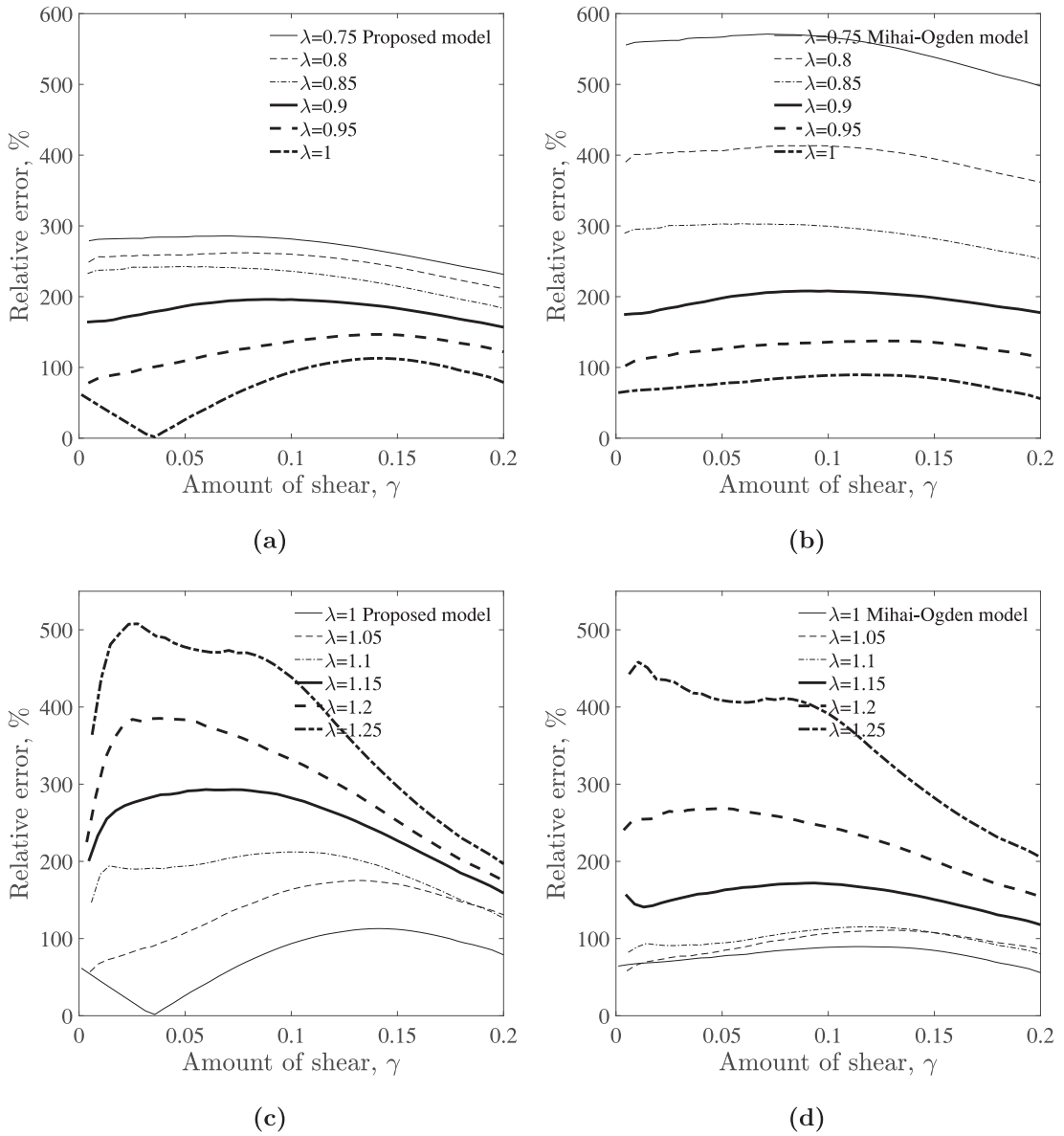

Fig. 5. Relative errors associated with shear stress T_{xz} during combined loading corresponding to the material parameters obtained in Section 4.4.

4.3. Predictions of the proposed and Mihai-Ogden model using data for simple shear

Shear stress in simple shear for the proposed model is computed to be

$$T_{xz} = \frac{1}{6\sqrt{\gamma^2+4}}\left(6\sqrt{2}a\left(\exp\left(\frac{b_0\left(\frac{6e^{\frac{1}{2}(b_1-\sqrt{3}b_1)}}{b_1}+\sqrt{7}+3\sqrt{3}-2\right)\tanh^{-1}\left(\frac{\gamma\sqrt{\gamma^2+4}}{\gamma^2+2}\right)}{6\sqrt{2}}\right)-1\right)\right.$$
$$\left.+\tanh^{-1}\left(\frac{\gamma\sqrt{\gamma^2+4}}{\gamma^2+2}\right)\left(ab_0\left(-\frac{6e^{\frac{1}{2}(b_1-\sqrt{3}b_1)}}{b_1}-\sqrt{7}-3\sqrt{3}+2\right)+6c\right)\right) \tag{65}$$

On applying traction-free boundary condition on a face of $5\text{mm}\times 5\text{mm}\times 5\text{mm}$ cubic specimen with its normal being in y-direction, i.e., $T_{yy}=0$, and by using Eq. (7), one arrives at the Lagrange multiplier p:

$$p = \gamma_1 N_{1yy} + \gamma_2 N_{2yy}. \tag{66}$$

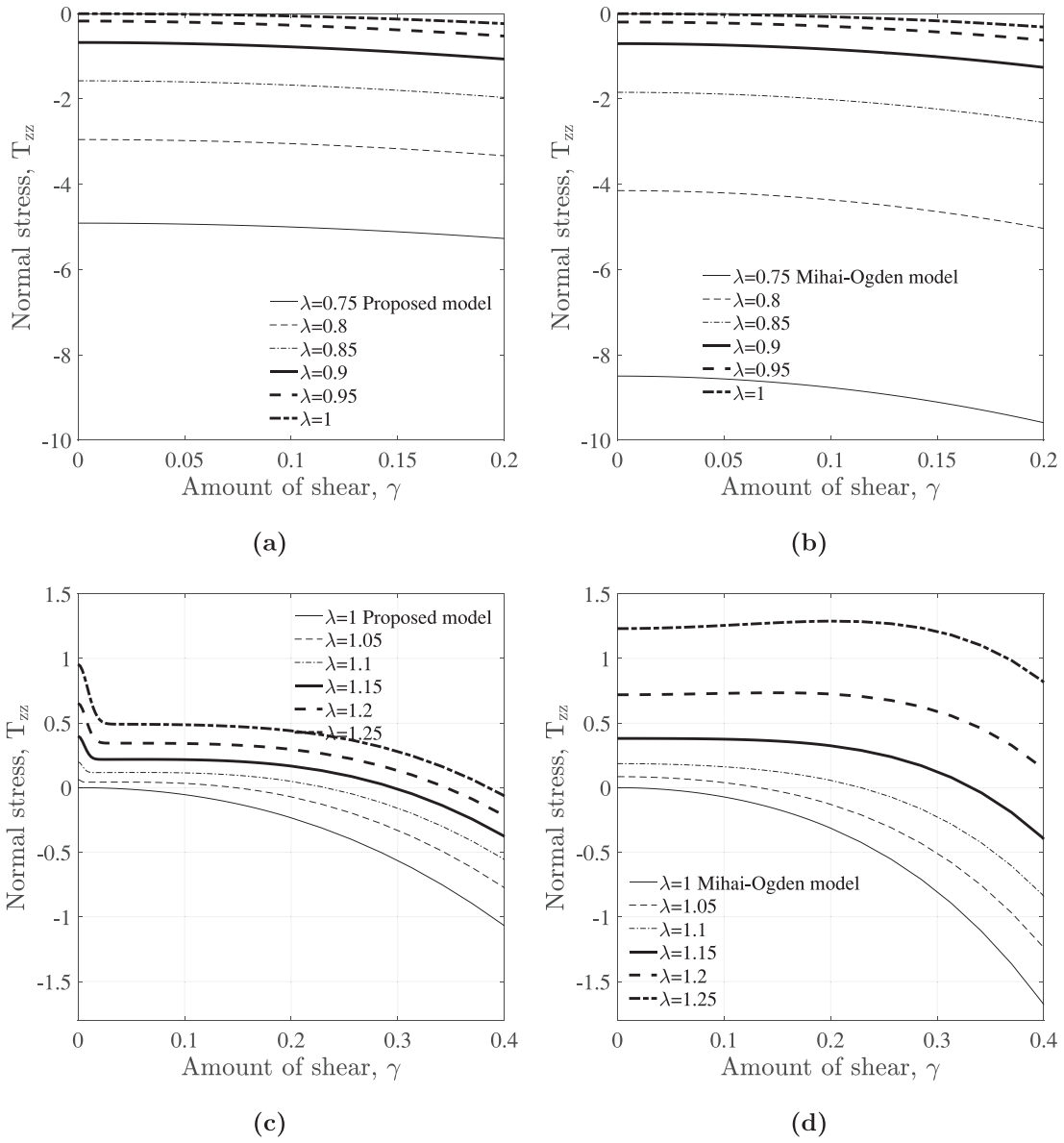

Fig. 6. Predicted normal stresses T_{zz} during combined loading using the material parameters obtained in Section 4.4.

where each symbol on the right hand side of the above equation can be computed using Eqs. (5), (9), (10), (17), (18) and (26). The multiplier corresponds to a combined tension/compression and shear. By substituting the Lagrange multiplier p in Eq. (7), one arrives at the three non-zero components of Cauchy stress interms of λ and γ, i.e,

$$T_{xx} = \gamma_1\left(N_{1xx} - N_{1yy}\right) + \gamma_2\left(N_{2xx} - N_{2yy}\right), \tag{67a}$$

$$T_{xz} = \gamma_1 N_{1xz} + \gamma_2 N_{2xz} \tag{67b}$$

and

$$T_{zz} = \gamma_1\left(N_{1zz} - N_{1yy}\right) + \gamma_2\left(N_{2zz} - N_{2yy}\right), \tag{67c}$$

By using the data for simple shear, the material parameters of the proposed and the Mihai-Ogden model are determined using differential evolution algorithm (refer to Table 1) by using all the three constraints discussed in the previous section, and checking the Hill inequality *a posteriori*. For the proposed model, the following constraints are used during the optimization process: $c > 0, a > 0, b_0 > 0, b_1 > 100$. The excellent fits associated with both models are plotted in Fig. 1. The predicted

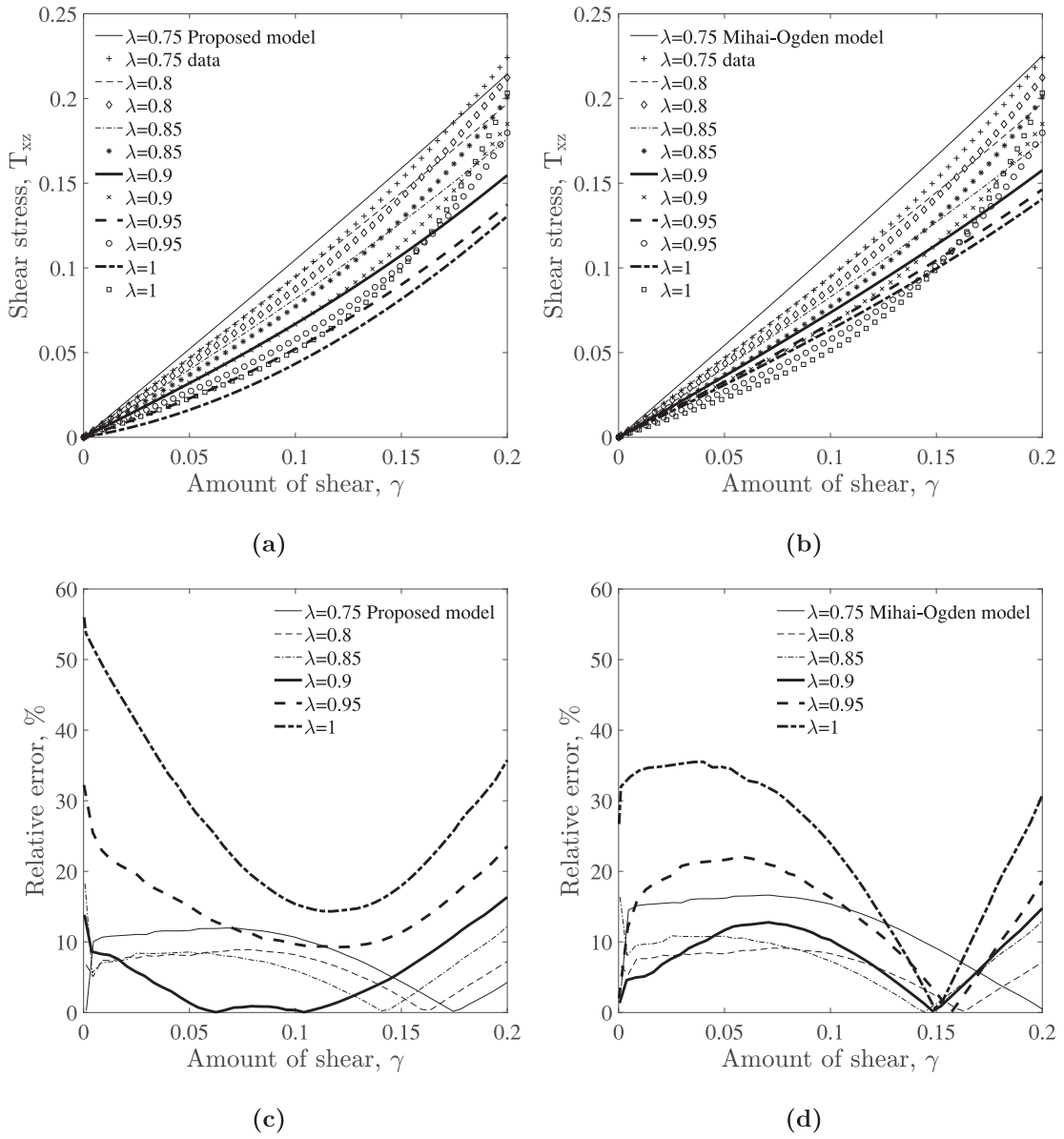

Fig. 7. Comparison of shear stresses for shear superposed on uniaxial compression.

normal and shear stresses during combined loading, i.e., uniaxial tension/compression followed by shear, are portrayed in Figs. 2 and 3, respectively. Notice that in Fig. 2d non-monotone Poynting stress T_{zz} is predicted for $\lambda = 1.05$ and $\lambda = 1.1$. In the absence of empirical inequality, T_{zz} for $\lambda = 1$ predicts adverse Poynting effect for a range of the parameter γ, contrary to that observed in experiments. Despite using the empirical inequality, the unexpected non-monotone behavior emerges for the other λ in tension and is not easy to control. Contrarily, for the proposed model, the monotone decreasing behavior of T_{zz} can be obtained by seeking appropriate values of the parameter b_1. The Fig. 2a and c associated with the proposed model show physically realistic monotone decreasing behavior. Interestingly, the calculated shear stresses connected with both the models for different degree of tension and compression, portrayed in Fig. 3, show nearly identical response.

4.4. Predictions using data for uniaxial response

The uniaxial response of the proposed and Mihai-Ogden model is fitted to the data for uniaxial deformation, and the extracted material parameters obtained for both the models are listed in Table 1. The best fits depicted in Fig. 4 show that Mihai-Ogden model emulates the data better than the proposed model. By using the same material parameters, the shear

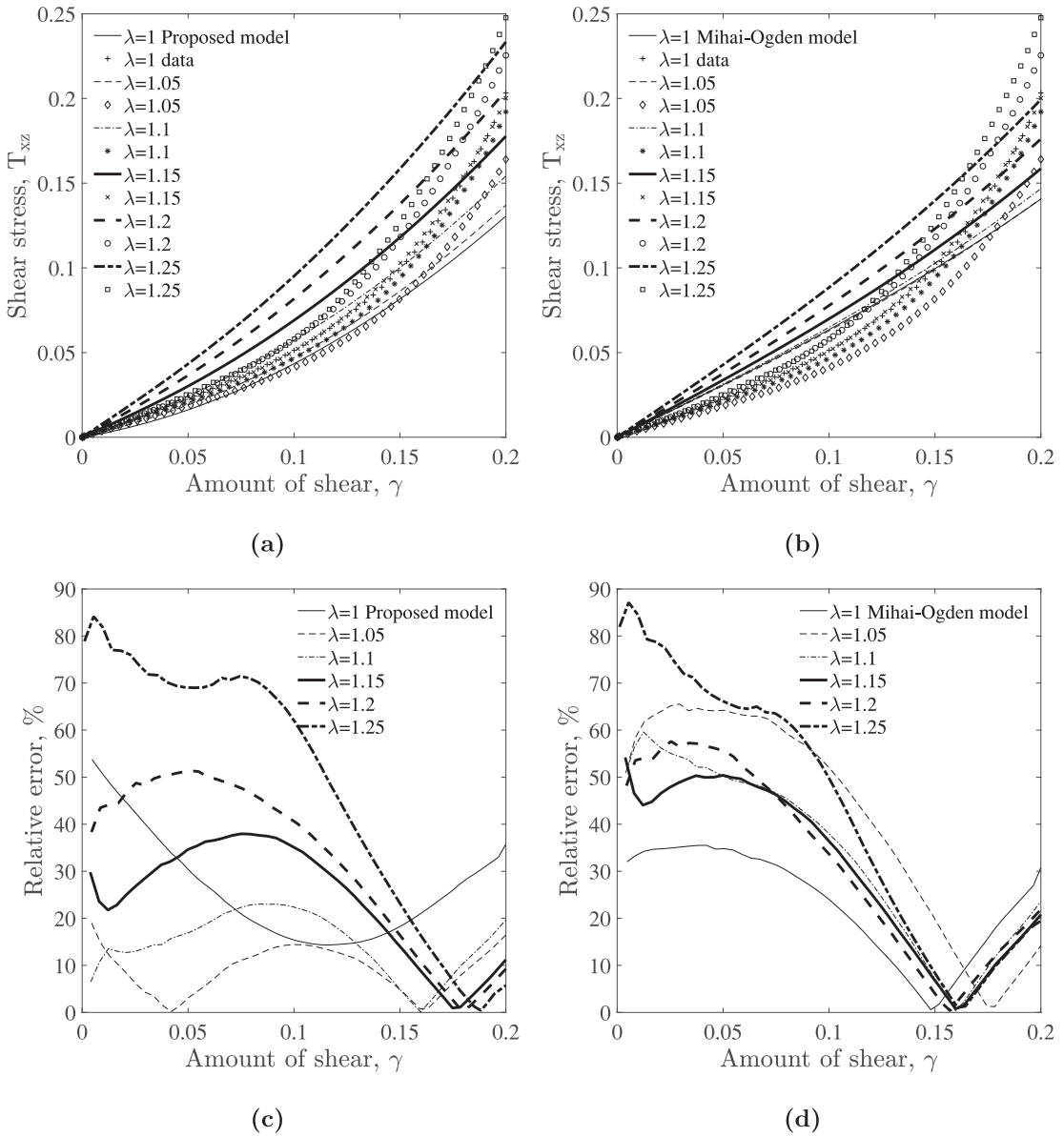

Fig. 8. Comparison of shear stresses for shear superposed on uniaxial tension.

response is predicted in combined loading conditions and compared with the experimental data. The relative errors are plotted in Fig. 5, which demonstrate that the predictions of the proposed model in combined compression and shear have a maximum error of about 300% as opposed to 600% for Mihai-Ogden model. However, in combined tension and shear, the errors associated with both the models are approximately the same. The predicted induced normal stresses related to Mihai-Ogden model, illustrated in Fig. 6d, show an unexpected non-monotone behavior for the stretches $\lambda = 1.2$ and $\lambda = 1.25$. On the other hand, the normal stresses predicted by the proposed model and plotted in Fig. 6 show a favorable response. Notice that in Fig. 6c the normal stresses T_{zz} fall-off rapidly due to the extreme value of the parameter $b_1 = 2748.05$. One can easily fix this issue when one caps the maximum value of $b_1 \approx 100$, at which point the mode function $\hat{b}(K_3)$ would have almost approached the limit function $b_0\left(\cos(K_3 + \frac{\pi}{6}) + \frac{\sqrt{7}-2}{6}\right)$ discussed in Section 3.4. The normal stresses in combined compression/tension and shear corresponding to the proposed model in Fig. 6a and c are bunched together in comparison with the Mihai-Ogden model because of the extreme values of b_1.

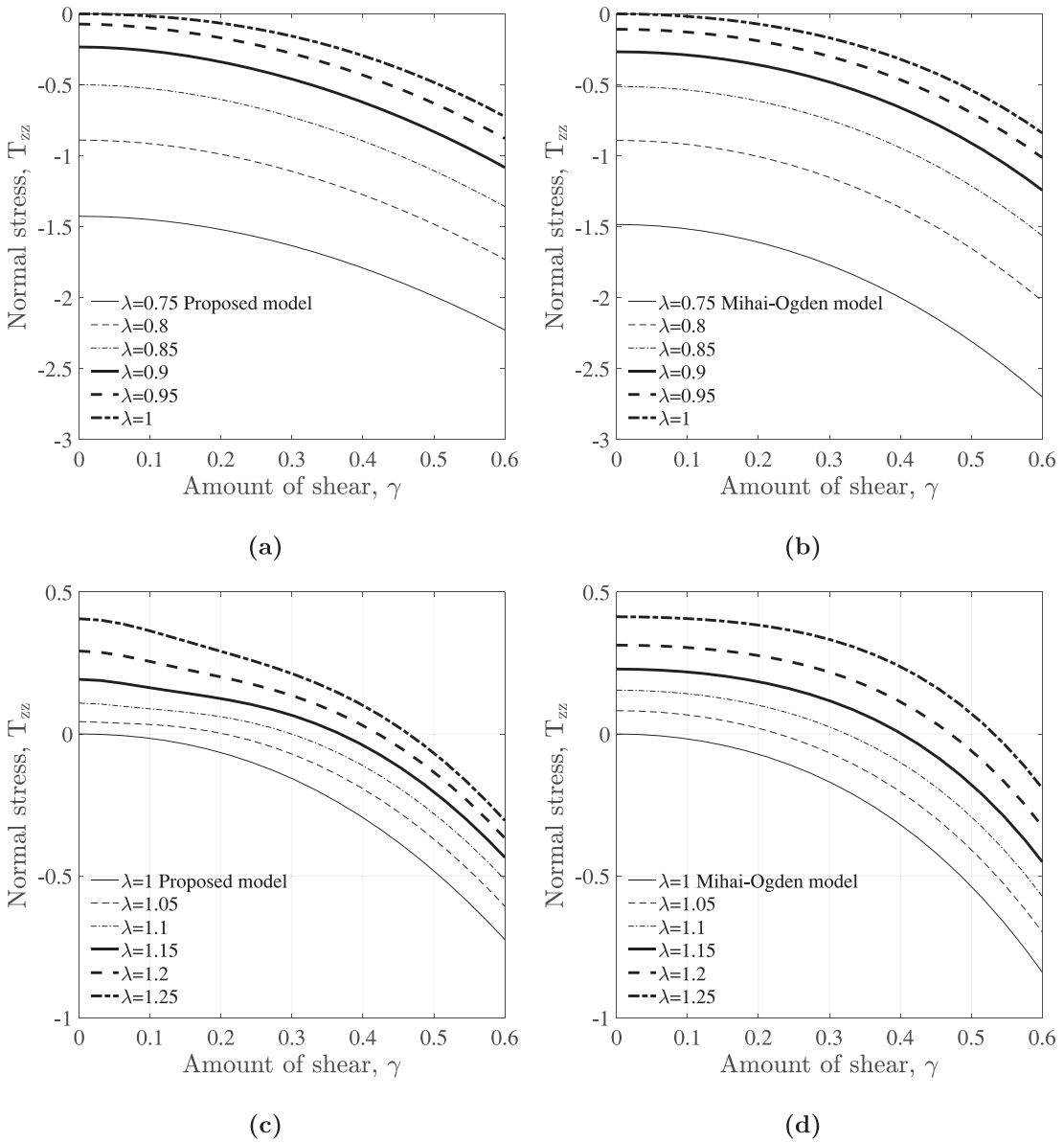

Fig. 9. Comparison of Poynting stresses T_{zz} for shear superposed on uniaxial deformation.

4.5. Predictions using data for combined compression/tension and shear

By using the Eqs. (64) and (67b), the predictions associated with Mihai-Ogden and the proposed model, respectively, are fitted to the measured shear stress in combined compression/tension and shear by employing the differential evolution algorithm. The resultant parameters are listed in Table 1. The Figs. 7 and 8 show the fit for different levels of compression and shear, and tension and shear, respectively. The relative errors in Fig. 7 indicate that both the models have similar quantitative behavior in compression. More importantly, the proposed model has a better qualitative response, in that the curvature is visible for the stretches $\lambda = 1$, $\lambda = 0.95$ and $\lambda = 0.9$ mimicking the data, while the response curves associated with Mihai-Ogden model only have nearly a linear response. The shear response in tension, portrayed in Fig. 8, affirm that the qualitative and quantitative predictions of the proposed model are better than that of Mihai-Ogden model. Notice that the curvature of the shear response is visible for the proposed model throughout the stretch range as opposed to nearly a linear response for Mihai-Ogden model. The corresponding normal stresses are plotted in Figs. 9 and 10. The Poynting stress T_{zz} show an expected monotone decreasing response for both the models, and the other normal stress T_{xx} shows a non-intersecting and intersecting responses for the proposed and the Mihai-Ogden model, respectively.

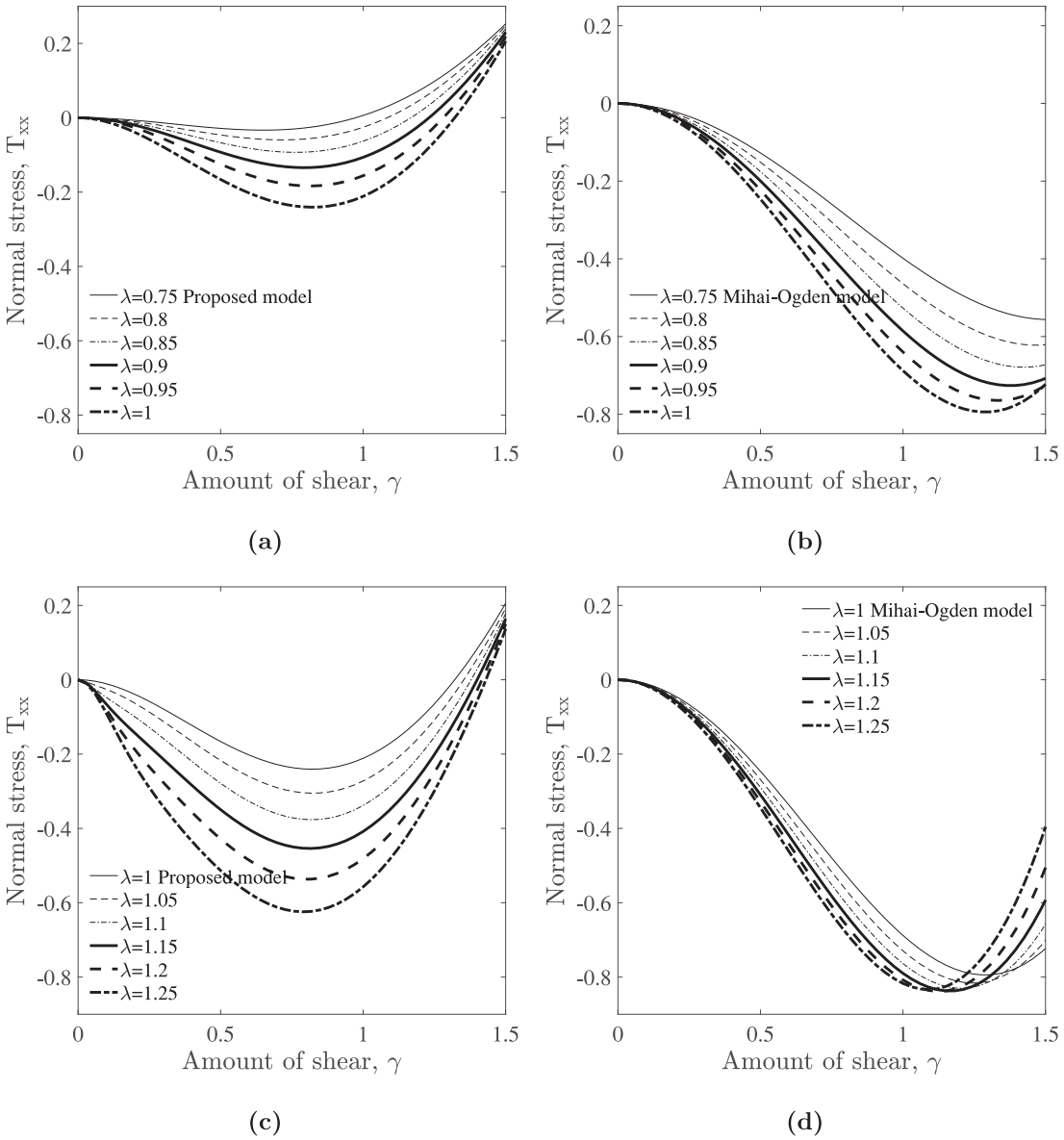

Fig. 10. Comparison of the normal stresses T_{xx} for shear superposed on uniaxial deformation.

In order to visualize the constructed potential vis-à-vis Mihai-Ogden model, the parameters associated with the combined loading is used and the constant potential curves are plotted in Fig. 11a. The isopotential curves are nearly identical and coincide for $W = 0.1$ except for the corners. For smaller values of the potential, the curves differ by a small amount. It is important to recognize that the stresses are related to the gradients of potential, and therefor small differences in (11 a) translate to substantial difference in stresses. The Fig. (11b) shows reasonably large domain where the equilibrium equations remain elliptic. On the other hand, Mihai-Ogden model remains elliptic in the entire domain. The deformation range over which the data measured by Budday et al. (2017) lies occupies a tiny region within the elliptic domain. The nine inequalities in theorem 6, which are necessary and sufficient, connected with any isotropic and incompressible material subjected to arbitrary deformation derived by Zubov and Rudev (2011) is used to plot the strong ellipticity domain. It may be interesting to note that (Zee and Sternberg, 1983) showed that the conditions of strong and ordinary ellipticity coalesce for Green elastic materials that are isotropic provided that Baker-Ericksen conditions are met and infinitesimal shear modulus is positive, both of which are satisfied for the proposed model.

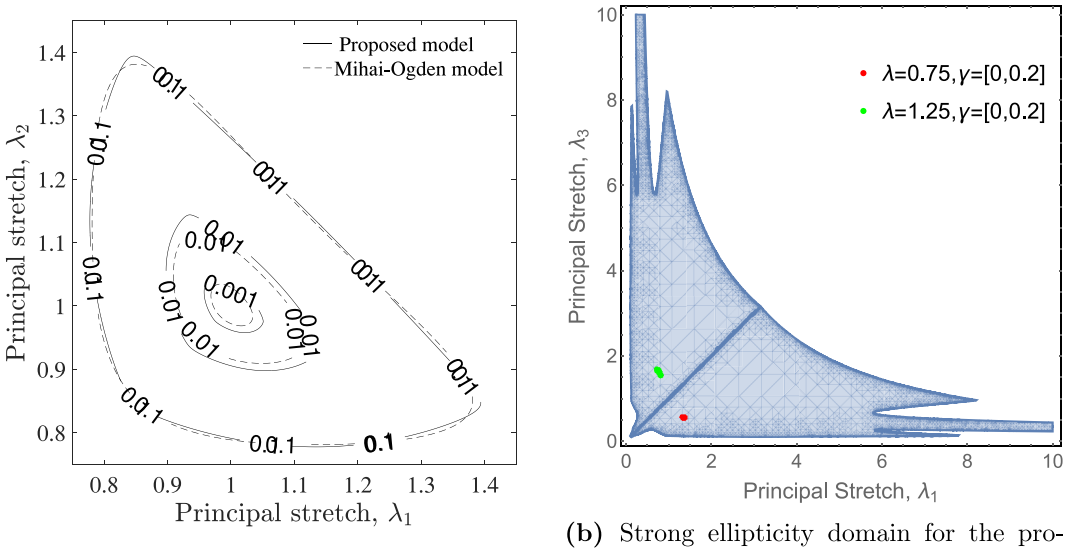

(a) Contour plots for potentials

(b) Strong ellipticity domain for the proposed potential

Fig. 11. The entire range of measurements made by Budday et al. (2017) occupies a small region of the panel on the right indicated by red and green dots. (For interpretation of the references to colour in this figure legend, the reader is referred to the web version of this article.)

5. Conclusions

The use of Lode invariants for hyperelastic formulations rendered *a priori* analysis using B-E inequalities and Hill inequality into a simple ordinary differential inequality, which are sequentially invoked to determine the functional form of the modulus function. Consecutively, the final form of the potential is also condensed. The use of any other non-orthogonal invariants may not be amenable to the analysis performed in this paper, and therefore extremely difficult to determine the mathematical form of the stored energy with those invariants. To the best of our knowledge, this is the first paper to partially determine the functional form of the potential in terms of the invariants characterizing the magnitude and mode of distortion using *a priori* analysis. For hyperelastic materials with higher modulus in compression compared to that in tension, we have established limits for the modulus function that satisfy B-E inequalities, and the constructed potential is capable of emulating every monotone decreasing modulus function in between those limits. The methodology developed in this paper can be applied to determine the stored energy function of collagenous biological tissues, which have a strong dependence on mode of distortion.

The domain of strong ellipticity is sufficiently large for the proposed model, within which classical solutions are embodied. When ellipticity is violated, our preliminary three and two dimensional simulations using the proposed potential show the emergence of necking-like phenomenon during extreme shearing of a block, and the appearance of localized shear banding during acute plane strain squeezing of a wedge, respectively. Interestingly, experiments on high rate of shearing of polybutadiene solution attributed to Tapadia and Wang (2003), Divoux et al. (2016) show the emergence of highly localized shear banding.

Appendix A. Rewriting the principal values of true strain in terms of the Lode invariants

Eqs. (19a) and (19b) are re-written in terms of sum and product of $\ln(\lambda_1)$ and $\ln(\lambda_2)$, i.e.,

$$\frac{K_2{}^2}{2} = \left(X^2 - Y\right) \tag{68a}$$

and

$$-K_2^3 \sin(3K_3) = 3\sqrt{6}XY, \tag{68b}$$

where $X = \ln(\lambda_1) + \ln(\lambda_2)$ and $Y = \ln(\lambda_1)\ln(\lambda_2)$.

By substituting the expression Y in Eq. (68b) and solving the resultant cubic equation in X with a positive discriminant, one arrives at three real solutions, i.e.,

$$X = \sqrt{\frac{2}{3}} K_2 \cos\left(K_3 + \frac{\pi}{6}\right), \tag{69a}$$

$$\sqrt{\frac{2}{3}}K_2\sin(K_3) \tag{69b}$$

and

$$\sqrt{\frac{2}{3}}K_2\cos(K_3-\frac{\pi}{6}). \tag{69c}$$

One arrives at a unique Y for each of the solutions (69), i.e., there are three pairs of solutions. For each pair X and Y, a quadratic equation in terms of $\ln(\lambda_1)$ with a positive discriminant produces two solutions, i.e.,

$$\ln(\lambda_1)=\frac{1}{2}\left(X-\sqrt{2K_2{}^2-3X^2}\right) \tag{70a}$$

and

$$\frac{1}{2}\left(X+\sqrt{2K_2{}^2-3X^2}\right), \tag{70b}$$

and the corresponding expression for $\ln(\lambda_2)$ is given through

$$\ln(\lambda_2)=\frac{1}{2}\left(X+\sqrt{2K_2{}^2-3X^2}\right) \tag{71a}$$

and

$$\frac{1}{2}\left(X-\sqrt{2K_2{}^2-3X^2}\right), \tag{71b}$$

respectively, In summary there are six pairs of solutions, i.e., six solutions for $\ln(\lambda_1)$ and its corresponding $\ln(\lambda_2)$. By substituting the six pairs in B-K inequalities (21) results in 18 inequalities with the coefficient of γ_2/γ_1 becoming independent of the invariant K_2. Further, each inequality in (21) produces the same three independent inequalities recorded in (22).

Appendix B. Eigenvectors of ln(V) and D coincide

The spectral representation of $\ln(\mathbf{V})$ and its derivative are as follows:

$$\ln(\mathbf{V})=\sum_{i=1}^{3}\ln(\lambda_i)\mathbf{n}_i\otimes\mathbf{n}_i \tag{72a}$$

and

$$\overline{\ln(\mathbf{V})}=\sum_{i=1}^{3}\left(\frac{\dot{\lambda}_i}{\lambda_i}\mathbf{n}_i\otimes\mathbf{n}_i+\ln(\lambda_i)\dot{\mathbf{n}}_i\otimes\mathbf{n}_i+\ln(\lambda_i)\mathbf{n}_i\otimes\dot{\mathbf{n}}_i\right). \tag{72b}$$

Since the eigenvectors of $\ln(\mathbf{V})$ are orthonormal, it immediately follows that

$$\mathbf{n}_i\cdot\mathbf{n}_j=\delta_{ij},\ \ i,j=1,2,3, \tag{73}$$

where δ_{ij} is the Kronecker delta. On differentiating the above equation, one arrives at

$$\dot{\mathbf{n}}_i.\mathbf{n}_i=0,\ \text{no sum on i} \tag{74a}$$

and

$$\dot{\mathbf{n}}_i.\mathbf{n}_j=-\mathbf{n}_i.\dot{\mathbf{n}}_j. \tag{74b}$$

From Eq. (74a) it is evident that the time derivative of each basis is perpendicular to the corresponding basis, and is a linear combination of the other two basis:

$$\dot{\mathbf{n}}_1=\alpha_{12}\mathbf{n}_2+\alpha_{13}\mathbf{n}_3, \tag{75a}$$

$$\dot{\mathbf{n}}_2=\alpha_{21}\mathbf{n}_1+\alpha_{23}\mathbf{n}_3 \tag{75b}$$

and

$$\dot{\mathbf{n}}_3=\alpha_{31}\mathbf{n}_1+\alpha_{32}\mathbf{n}_2. \tag{75c}$$

Notice that $\alpha_{ij}=0$ whenever $i=j$. On using Eqs. (74) and (75), one obtains

$$\alpha_{21}=-\alpha_{12},\alpha_{32}=-\alpha_{23}\ \text{and}\ \alpha_{31}=-\alpha_{13}. \tag{76}$$

Since the α_{ij}'s form a skew-symmetric matrix, one can rewrite Eq. (75) as follows:

$$\dot{\mathbf{n}}_i = \sum_{p=1}^{3} W_{ip}\mathbf{n}_p, \quad i = 1, 2, 3, \tag{77}$$

where the α_{ij}'s form the components of the skew-symmetric matrix W_{ij}. By substituting Eq. (77) in Eq. (72b), one arrives at

$$\overset{\cdot}{\overline{\ln(\mathbf{V})}} = \frac{\dot{\lambda}_i}{\lambda_i}\mathbf{n}_i \otimes \mathbf{n}_i + \ln(\lambda_i)W_{ip}\mathbf{n}_p \otimes \mathbf{n}_i + \ln(\lambda_i)\mathbf{n}_i \otimes W_{ip}\mathbf{n}_p. \tag{78}$$

Starting from the above equation, Einstein's summation assumption is in effect. Rewriting the above results in

$$\overset{\cdot}{\overline{\ln(\mathbf{V})}} = \frac{\dot{\lambda}_i}{\lambda_i}\mathbf{n}_i \otimes \mathbf{n}_i + W_{qp}(\mathbf{n}_p \otimes \mathbf{n}_q)\delta_{ij}\ln(\lambda_i)(\mathbf{n}_i \otimes \mathbf{n}_j) + \delta_{ij}\ln(\lambda_i)(\mathbf{n}_i \otimes \mathbf{n}_j)W_{qp}(\mathbf{n}_q \otimes \mathbf{n}_p). \tag{79}$$

The total material derivative of $\ln(\mathbf{V})$ derived by Xiao et al. (1997) reads as

$$\overset{\cdot}{\overline{\ln(\mathbf{V})}} = \mathbf{D} + \boldsymbol{\Omega}^{\ln}\ln(\mathbf{V}) - \ln(\mathbf{V})\boldsymbol{\Omega}^{\ln}, \tag{80}$$

where $\boldsymbol{\Omega}^{\ln}$ is the logarithmic spin tensor. By comparing Eq. (79) with that of Eq. (80), Eq. (79) can be rewritten in tensor form as

$$\overset{\cdot}{\overline{\ln(\mathbf{V})}} = \mathbf{D} + \mathbf{W}^{\mathrm{T}}\ln(\mathbf{V}) - \ln(\mathbf{V})\mathbf{W}^{\mathrm{T}}. \tag{81}$$

Therefore, $\ln(\mathbf{V})$ and $\mathbf{D}$ have the same eigenvectors.

Appendix C. Hill stability of Hencky strain based incompressible hyperelastic materials

The principal values of the extra part of the Cauchy stress t_i^e, $i = 1, 2, 3$, is related to the potential function W through

$$t_i^e(\ln\lambda_1, \ln\lambda_2, -\ln\lambda_1 - \ln\lambda_2) = \frac{\partial W}{\partial \ln\lambda_i}(\ln\lambda_1, \ln\lambda_2, \ln\lambda_3)\Big|_{\ln\lambda_3 = -\ln\lambda_1 - \ln\lambda_2}, \quad i = 1, 2, 3. \tag{82}$$

Eq. (30) is rewritten using the spectral representations of the extra part of Cauchy stress $\mathbf{T}^e$ and the symmetric part of the velocity gradient $\mathbf{D}$, i.e.,

$$\overset{\cdot}{\overline{t_i^e(\mathbf{n}_i \otimes \mathbf{n}_i)}} \cdot \frac{\dot{\lambda}_j}{\lambda_j}(\mathbf{n}_j \otimes \mathbf{n}_j) \geq 0. \tag{83}$$

By expanding the above equation, and on using $\dot{\mathbf{n}}_i \cdot \mathbf{n}_i = 0$ one arrives at the following inequality:

$$\frac{\partial t_i^e}{\partial \ln\lambda_j}\left(\frac{\dot{\lambda}_j}{\lambda_j}\right)\left(\frac{\dot{\lambda}_i}{\lambda_i}\right) \geq 0. \tag{84}$$

On substituting Eq. (82) in Eq. (84) results in

$$\frac{\partial^2 W}{\partial \ln\lambda_i \partial \ln\lambda_j}\Bigg|_{\ln\lambda_3 = -\ln\lambda_1 - \ln\lambda_2}\left(\frac{\dot{\lambda}_j}{\lambda_j}\right)\Bigg|_{\frac{\dot{\lambda}_3}{\lambda_3} = -\frac{\dot{\lambda}_1}{\lambda_1} - \frac{\dot{\lambda}_2}{\lambda_2}}\left(\frac{\dot{\lambda}_i}{\lambda_i}\right)\Bigg|_{\frac{\dot{\lambda}_3}{\lambda_3} = -\frac{\dot{\lambda}_1}{\lambda_1} - \frac{\dot{\lambda}_2}{\lambda_2}} \geq 0. \tag{85}$$

Eq. (85) is of the following form:

$$H_{ij}v_j v_i \geq 0, \tag{86}$$

where H is Hessian matrix with respect to the principal values of Hencky strain. Notice that the Hessian is to be computed assuming W to be a function of $\ln(\lambda_1)$, $\ln(\lambda_2)$ and $\ln(\lambda_3)$ and applying the incompressibility constraint a posteriori. In order to determine whether the potential (47) is Hill-stable or not, one needs to use the definition of invariants recorded in (4), rewrite the potential in terms of the principal values of Hencky strain and determine its Hessian with respect to the principal values.

References

Abeyaratne, R.C., 1980. Discontinuous deformation gradients in plane finite elastostatics of incompressible materials. J. Elast. 10 (3), 255–293.
Baker, M., Ericksen, J., 1954. Inequalities restricting the form of the stress-deformation relations for isotropic elastic solids and Reiner-Rivlin fluids. J. Washington Acad. Sci. 44 (2), 33–35.
Balbi, V., Trotta, A., Destrade, M., Annaidh, A.N., 2019. Poynting effect of brain matter in torsion. Soft matter Royal Society of Chemistry.
Boyce, M.C., Arruda, E.M., 2000. Constitutive models of rubber elasticity: a review. Rubber Chem. Technol. 73 (3), 504–523.
Budday, S., Sommer, G., Birkl, C., Langkammer, C., Haybaeck, J., Kohnert, J., Bauer, M., Paulsen, F., Steinmann, P., Kuhl, E., et al., 2017. Mechanical characterization of human brain tissue. Acta Biomater. 48, 319–340.
Chagnon, G., Rebouah, M., Favier, D., 2015. Hyperelastic energy densities for soft biological tissues: a review. J. Elast. 120 (2), 129–160.

Chen, M., Tan, Y., Wang, B., 2012. General invariant representations of the constitutive equations for isotropic nonlinearly elastic materials. Int. J. Solids Struct. 49 (2), 318–327.
Criscione, J.C., Humphrey, J.D., Douglas, A.S., Hunter, W.C., 2000. An invariant basis for natural strain which yields orthogonal stress response terms in isotropic hyperelasticity. Int. J. Solids Struct. 48 (12), 2445–2465.
Dacorogna, B., 2001. Necessary and sufficient conditions for strong ellipticity of isotropic functions in any dimension. Discrete Continuous Dyn. Syst. Ser.B 1 (2), 257–263.
Destrade, M., Gilchrist, M., Murphy, J.G., Rashid, B., Saccomandi, G., 2015. Extreme softness of brain matter in simple shear. Int. J. Non-Linear Mech. 75, 54–58.
Divoux, T., Fardin, M.A., Manneville, S., Lerouge, S., 2016. Shear banding of complex fluids. Annu. Rev. Fluid Mech. 48, 81–103.
Goriely, A., Budday, S., Kuhl, E., 2015. Neuromechanics: from neurons to brain. In: Advances in Applied Mechanics, Vol. 48. Elsevier, pp. 79–139.
Hill, R., 1970. Constitutive inequalities for isotropic elastic solids under finite strain. Proc. R. Soc. London A. 314 (1519), 457–472.
Humphrey, J.D., 2003. Continuum biomechanics of soft biological tissues. Proc R Soc London Ser.A 459 (2029), 3–46.
Jog, C., Patil, K.D., 2013. Conditions for the onset of elastic and material instabilities in hyperelastic materials. Arch. Appl. Mech. 83 (5), 661–684.
Knowles, J.K., Sternberg, E., 1976. On the failure of ellipticity of the equations for finite elastostatic plane strain. Arch. Ration. Mech. Anal. 63 (4), 321–336.
Marckmann, G., Verron, E., 2006. Comparison of hyperelastic models for rubber-like materials. Rubber Chem. Technol. 79 (5), 835–858.
Marsden, J.E., Hughes, T.J., 1994. Mathematical Foundations of Elasticity. Courier Corporation.
Martin, R.J., Ghiba, I.-D., Neff, P., 2018. A non-ellipticity result, or the impossible taming of the logarithmic strain measure. Int. J. Non-Linear Mech. 102, 147–158.
Marzano, S., 1983. An interpretation of Baker-Ericksen inequalities in uniaxial deformation and stress. Meccanica 18 (4), 233–235.
Mihai, L.A., Chin, L., Janmey, P.A., Goriely, A., 2015. A comparison of hyperelastic constitutive models applicable to brain and fat tissues. J. R. Soc. Interface 12 (110), 20150486.
Mihai, L.A., Budday, S., Holzapfel, G.A., Kuhl, E., Goriely, A., 2017. A family of hyperelastic models for human brain tissue. Int. J. Solids Struct. 106, 60–79.
Mihai, L.A., Goriely, A., 2011. Positive or negative poynting effect? The role of adscititious inequalities in hyperelastic materials. Proc. R. Soc. A 467 (2136), 3633–3646.
Mihai, L.A., Goriely, A., 2017. How to characterize a nonlinear elastic material? A review on nonlinear constitutive parameters in isotropic finite elasticity. Proc. R. Soc. A 473 (2207), 20170607.
Monigari, K., Kannan, K., 2013. A class of models to predict the normal force and torque under torsional loading of a viscoelastic liquid. Int. J. Eng. Sci. 71, 80–91.
Neff, P., Ghiba, I.-D., Lankeit, J., 2015. The exponentiated Hencky-logarithmic strain energy. Part i: constitutive issues and rank-one convexity. J. Elast. 121 (2), 143–234.
Ogden, R.W., 1972. Large deformation isotropic elasticity–on the correlation of theory and experiment for incompressible rubberlike solids. Proc. R. Soc. Lond. A 326 (1567), 565–584.
Rivlin, R.S., 2004. Restrictions on the strain-energy function for an elastic material. Math. Mech. Solids 9 (2), 131–139.
de Rooij, R., Kuhl, E., 2016. Constitutive modeling of brain tissue: current perspectives. Appl. Mech. Rev. 68 (1), 010801.
Sendova, T., Walton, J.R., 2005. On strong ellipticity for isotropic hyperelastic materials based upon logarithmic strain. Int. J. Non-Linear Mech. 40 (2–3), 195–212.
Sidoroff, F., 1974. Sur les restrictionsa imposera lâ;;énergie de déformation dâ;;un matériau hyperélastique. C. R. Acad. Sci. 279, 379–382.
Silhavy, M., 2013. The Mechanics and Thermodynamics of Continuous Media. Springer Science & Business Media.
Tapadia, P., Wang, S.-Q., 2003. Yieldlike constitutive transition in shear flow of entangled polymeric fluids. Phys. Rev. Lett. 91 (19), 198301.
Truesdell, C., Noll, W., 2004. The non-linear field theories of mechanics. In: The Non-Linear Field Theories of Mechanics. Springer, pp. 1–579.
Wex, C., Arndt, S., Stoll, A., Bruns, C., Kupriyanova, Y., 2015. Isotropic incompressible hyperelastic models for modelling the mechanical behaviour of biological tissues: a review. Biomed. Eng. 60 (6), 577–592.
Wineman, A., Gandhi, M., 1984. On local and global universal relations in elasticity. J. Elast. 14 (1), 97–102.
Xiao, H., Bruhns, O., Meyers, A., 1997. Logarithmic strain, logarithmic spin and logarithmic rate. Acta Mech. 124 (1–4), 89–105.
Zee, L., Sternberg, E., 1983. Ordinary and strong ellipticity in the equilibrium theory of incompressible hyperelastic solids. Arch. Ration. Mech. Anal. 83 (1), 53–90.
Zubov, L., Rudev, A., 2011. A criterion for the strong ellipticity of the equilibrium equations of an isotropic non-linearly elastic material. J. Appl. Math. Mech. 75 (4), 432–446.